

CATEGORY *C-44a*

DOCUMENT NO.

HW-31351

DECLASSIFIED**GENERAL  ELECTRIC**

HANFORD ATOMIC PRODUCTS OPERATION - RICHLAND, WASHINGTON

DATE

April 5, 1954

COPY NO. AND SERIES

☒

RESTRICTED DATA

THIS DOCUMENT CONTAINS RESTRICTED DATA AS
DEFINED IN THE ATOMIC ENERGY ACT OF 1946.
IT IS PROHIBITED TO TRANSMIT OR DISCLOSE ITS
CONTENTS IN ANY MANNER TO AN UNAUTHORIZED
PERSON OR PERSONS PROHIBITED.

FILE DESIGNATION

300 N

TITLE

QUARTERLY REPORT, PHYSICS UNIT
January, February, March, 1954

AUTHOR

The Staff of the Physics Unit

☐ OTHER SPECIAL CLASSIFIED INFORMATION
THIS MATERIAL CONTAINS INFORMATION AFFECTING
THE NATIONAL DEFENSE OF THE UNITED STATES
WITHIN THE MEANING OF THE ESPIONAGE LAWS,
TITLE 18, U. S. C., SECTIONS 793 AND 794, THE TRANSMISSION
OR REVELATION OF WHICH IN ANY MANNER
TO AN UNAUTHORIZED PERSON IS PROHIBITED BY
LAW.

THIS DOCUMENT IS NOT TO BE LEFT UNATTENDED WHERE AN UNAUTHORIZED PERSON MAY HAVE ACCESS
TO IT. WHEN NOT IN USE, IT MUST BE STORED IN AN APPROVED LOCKED CONTAINER WITHIN AN APPROVED
GUARDED AREA, WHILE IT IS IN YOUR POSSESSION AND UNLESS YOU HAVE OBTAINED A SIGNED RECEIPT
CLASSIFYING IT. IT IS YOUR RESPONSIBILITY TO KEEP IT AND ITS CONTENTS WITHIN THE LIMITS OF
THIS PROJECT. IF FROM AN UNAUTHORIZED PERSON, ITS TRANSFER, TO, AND STORAGE IN YOUR PLACE
OF RESIDENCE IS PROHIBITED. IT IS NOT TO BE DUPLICATED. ADDITIONAL COPIES ARE REQUIRED,
OBTAIN THEM FROM THE RELATIONSHIP FILE. ALL PERSONS READING THIS DOCUMENT ARE REQUESTED
TO SIGN IN THE SPACE PROVIDED BELOW.

ROUTE TO:

READ BY:

DATE

ROUTE TO:

READ BY:

DATE

*R. E. Harrison**P. Lippincott* 32563

318

MAY 29 1954

INVENTORIED
FEB 21 1955

RESTRICTED DATA
THIS DOCUMENT CONTAINS RESTRICTED DATA AS
DEFINED IN THE ATOMIC ENERGY ACT OF 1946.
IT IS PROHIBITED TO TRANSMIT OR DISCLOSE ITS
CONTENTS IN ANY MANNER TO AN UNAUTHORIZED
PERSON OR PERSONS PROHIBITED.
TO ADMINISTER AND CRIMINAL SANCTIONS.

THIS DOCUMENT IS PUBLICLY
AVAILABLE

DECLASSIFIED

C-3195-MS (5-53)
A.E.C.-G.E.-RICHLAND, WASH.

DECLASSIFIED

DECLASSIFIED

GENERAL ELECTRIC
COMPANY

-1-

HW-31351

Reactors - Production

RICHLAND, WASHINGTON

HANFORD ATOMIC PRODUCTS OPERATION

WARNING - PRELIMINARY REPORT

THIS REPORT CONTAINS INFORMATION OF A PRELIMINARY NATURE AND IS PREPARED PRIMARILY FOR THE USE OF HANFORD WORKS TECHNICAL DIVISIONS PERSONNEL. THIS REPORT IS SUBJECT TO REVISION ON FURTHER CHECKING OR COLLECTION OF ADDITIONAL DATA.

QUARTERLY REPORT

PHYSICS UNIT

JANUARY, FEBRUARY, MARCH, 1954

by

The Staff of the Physics Unit

Applied Research Sub-Section, Technical Section
ENGINEERING DEPARTMENT

April 5, 1954

CLASSIFICATION CANCELLED AND CHANGED TO

DECLASSIFIED

BY AUTHORITY OF RM HerPR-24 7-2-92BY DB Burk 9-9-92VERIFIED BY DK Hanson, 9-9-92

Hanford Atomic Products Operation
General Electric Company
Richland, Washington

DECLASSIFIED

This document consists of
50 pages. Copy No. 25
of 133 copies. Series [redacted]

Classified by [redacted] to

UNCL

By

By Authority of [redacted]

3/8/82, [redacted] dated
[redacted] Doc,
[redacted] 12/20/84

This document contains restricted data as defined
in the Atomic Energy Act of 1954. Its trans-
mission or the use of its contents in any manner to
an unauthorized person is prohibited.

RESTRICTED DATA

THIS DOCUMENT CONTAINS RESTRICTED DATA
AS DEFINED IN THE ATOMIC ENERGY ACT OF
1954. UNAUTHORIZED DISCLOSURE SUBJECT
TO ADMINISTRATIVE AND CRIMINAL SANCTIONS.

DECLASSIFIED

A PRIME CONTRACTOR FOR THE U.S. ATOMIC ENERGY COMMISSION

Reactors - Production

INTERNAL DISTRIBUTIONCopy Number

1. FW Albaugh
2. PM Anselone - WC McGee
3. RE Beaton
4. CA Bennett
5. EZ Block
6. J Braunstein
7. LP Bupp
8. AH Bushey - RJ Brouns - HR Schmidt - HH Hopkins
9. JJ Cadwell - OJ Wick
10. JC Chatten
11. ED Clayton
12. RK Cole
13. DE Davenport
14. MV Davis - HA Fowler
15. RL Dickeman - WK Alexander
16. DJ Donahue - DD Lanning
17. JO Erkman
18. WB Farrand
19. JE Faulkner
20. PF Gast
21. OH Greager
22. AB Greninger
23. RB Hamilton - DE Crouter
24. SM Hauser
→ 25. RE Heineman
26. KW Hess
27. WA Horning
28. HW Lefevre
29. FJ Leitz
30. BR Leonard
31. WR Lewis
32. RC Lloyd
33. GE McCullough
34. RE McGrath
35. EB Montgomery - JW Hall
36. GM Muller
37. H Neumann
38. JD Orton
39. GF Owsley - PC Walkup
40. WJ Ozeroff
41. RE Peterson
42. RP Raftery
43. PH Reinker - MW Carbon
44. RB Richards
45. CR Richey
46. JE Robb - SR Stamp - RE Dunn

DECLASSIFIED**DECLASSIFIED**

Reactors - Production

INTERNAL DISTRIBUTION (contd.)Copy Number**DECLASSIFIED**

47 GM Roy
 48 GF Scott - PG Holsted
 49 EJ Seppi
 50 WP Stinson
 51 GW Stuart
 52 JR Triplett
 53 LD Turner
 54 AP Vinther - RR Bloomstrand - JB Czirr
 55 JH Warren - RO Mehann
 56 WW Windsheimer
 57 RW Woodruff
 58 WK Woods
 59 300 Files
 60 Yellow Copy

EXTERNAL DISTRIBUTIONCopy Number

61 - 70 Argonne National Laboratory
 71 Argonne National Laboratory, Attn: J. M. West
 72 Armed Forces Special Weapons Project, Washington
 73 - 77 Atomic Energy Commission, Washington
 78 Battelle Memorial Institute
 79 Brookhaven National Laboratory, Attn: J. Chernick
 80 Brookhaven National Laboratory, Attn: J. A. Harvey
 81 Bureau of Ships
 82 California Research and Development Company
 83 - 88 Carbide and Carbon Chemicals Company (ORNL)
 89 Chicago Patent Group
 90 - 93 duPont Company, Augusta
 94 duPont Company, Augusta, Attn: C.W.J. Wende
 95 duPont Company, Wilmington
 96 Hanford Operations Office
 97 - 98 Knolls Atomic Power Laboratory
 99 Knolls Atomic Power Laboratory, Attn: L. Tonks
 100 - 101 Los Alamos Scientific Laboratory
 102 Massachusetts Institute of Technology (Benedict)
 103 - 104 New York Operations Office
 105 North American Aviation, Inc.
 106 North American Aviation, Inc., Attn: S. Siegel
 107 Patent Branch, Washington
 108 - 111 Phillips Petroleum Company
 112 San Francisco Operations Office
 113 - 114 University of California Radiation Laboratory, Berkeley
 115 - 116 Westinghouse Electric Corporation
 117 - 118 University of California Radiation Laboratory, Livermore
 119 - 133 Technical Information Service, Oak Ridge

DECLASSIFIED

TABLE OF CONTENTS

DECLASSIFIED

	Page No.
SUMMARY	6
LATTICE PHYSICS	6
Calculation of Thermal Neutron Behavior in a Solid Cylindrical Fuel Rod - G. W. Stuart and R. W. Woodruff.....	6
I. Introduction.....	6
II. Calculations.....	7
A. Collision Densities.....	7
B. Collision Probabilities.....	9
C. Blackness.....	11
D. Average Angle of Escape.....	11
III. Conclusion.....	12
Computations for Transport Theory - G. M. Muller.....	13
The Solution of Boltzmann's Equation with the Aid of Functions Orthogonal on a Hemisphere - W. A. Horning.....	14
Measurement of Uranium Resonance for Use in Small-Source Theory - R. K. Cole.....	14
Exponential Pile Measurements in Graphite-Uranium Lattices - E. D. Clayton, C. R. Richey and E. Z. Block.....	18
I. 1.66" O.D., 1.10" I.D. Hollow Slug.....	18
II. Effect of Cooling Annulus on Buckling.....	18
III. Cross-Over Buckling.....	20
Correlation of Buckling Measurements and Theoretical Formulas - D. E. Davenport.....	20
Exponential Measurements in 4' x 4' Exponential Piles - W. B. Farrand and R. C. Lloyd.....	23
I. Relocation of Exponential Facilities.....	23
II. 4' x 4' Exponential Piles.....	24
III. Polonium-Beryllium Source Calibrations.....	24
IV. Flux Traverses within a Lattice Cell of the 8-3/8" Lattice.	24
V. Uranium Lattice Measurements.....	25
Physical Constants Testing Reactor - D. J. Donahue and D. D. Lanning.....	25
I. Nuclear Safety Considerations.....	25
II. Critical Mass of the Physical Constants Testing Reactor,...	26

DECLASSIFIED

DECLASSIFIED

TABLE OF CONTENTS (contd)

	<u>Page No.</u>
NUCLEAR PHYSICS.....	38
Development of a Technique for Measuring the Conversion Ratio for U-233 Production in Exponential Pile Experiments - W. P. Stinson and H. W. Lefevre.....	38
Neutron Spectrometer Facilities - B. R. Leonard, Jr., and E. J. Seppi	38
I. The Energy Variation of Alpha of U-235.....	38
II. Higher Order Corrections.....	39
A Study of the Error Associated with Neutron Cross Sections Calcu- lated from Empirical Formulas - E. J. Seppi.....	39
Thermal Neutron Temperatures - R. E. Heineman.....	42
C-12 Absorption Cross Section Measurement - R. E. Peterson.....	43
Pu-240 Burnout Experiments - D. J. Donahue and J. E. Faulkner.....	43
PHYSICS PROBLEMS CONNECTED WITH PLANT OPERATION.....	44
The Dependence of Pu-240 Concentration in Pile Produced Plutonium on Neutron Flux Level - B. R. Leonard, Jr.....	44
Neutron Sources - J. O. Erkman.....	47
Increasing the Subcritical Flux in a Hanford Reactor - J. O. Erkman..	47
Xenon Reactivity Effects - J. O. Erkman.....	48
Single Reactor Load for Tritium and Uranium-233 Production - G. W. Stuart.....	48
Conversion Ratio of Thoria - G. W. Stuart.....	49
Conversion Ratio for P-10 Production - R. E. Peterson.....	49
Production of Th-234 and Pa-233 - J. T. Russell.....	50
Wide Range Flux Meter - J. T. Russell.....	50

DECLASSIFIED

DECLASSIFIEDSUMMARY

A new method of calculating neutron distributions in a cylinder which has appreciable absorption is described. Measurements and calculations on the small-source theory treatment of resonance absorption in U-238 are given. Experimental measurements are reported of the bucklings of lattices utilizing hollow uranium slugs. The effects of varying amounts of cooling water in a graphite-uranium lattice have been measured. A detailed mathematical fitting of experimental reactivity data has been started; some initial results are given here. Curves showing the periods of the lattice testing reactor under various conditions have been calculated in connection with a study of the nuclear safety of this reactor. A method for calculating the critical mass and an estimate (4.4 kg of U-235) thereof is presented.

A technique for measuring the conversion efficiency for U-233 production of Hanford-type lattices is being developed. In connection with the study of the temperature coefficient of reactivity, an analysis has been made of the errors in reactivity change estimates produced by errors in cross-section measurements.

The dependence of Pu-240 content in product plutonium on the flux level at which irradiation takes place, which is produced by the 23-day half life of Np-239 is worked out in some detail. An experiment for assisting the design of an internal source for Hanford piles is outlined. A possible pile load capable of simultaneous U-233 and tritium production is described. A comparison of the conversion efficiencies of thorium metal and thorium oxide is given. Based on some recent production data, a new estimate of 0.65 for the tritium conversion efficiency is obtained. This figure includes separations losses.

LATTICE PHYSICS

Calculation of Thermal Neutron Behavior in a Solid Cylindrical Fuel Rod -
G. W. Stuart and R. W. Woodruff

I. Introduction

The purpose of the following work is to outline a method for calculating various quantities which describe the behavior of thermal neutrons within a solid cylindrical fuel rod. The basis for the method is a Monte Carlo calculation by D. D. McCracken and G. M. Muller which indicates that the angular distribution of thermal neutrons incident on an absorber contained in a reasonable amount of moderator is hemispherically symmetric. This information coupled with a knowledge of the scattering and absorption cross sections of the fuel rod makes possible the calculation of the distribution of thermal neutrons within the rod, the blackness of the rod to thermal neutrons, and the average angle of escape of these neutrons. To this end, it is first necessary to find the collision density per unit time of each neutron generation and the probability that a neutron of a given generation will suffer at least one more collision before escape.* The generations are distinguished by the number of collisions suffered

* This is the technique traditionally used to calculate the fast effect.

DECLASSIFIED

subsequent to entering the fuel rod; thus the n th generation neutrons have had n collisions.

II. Calculations

DECLASSIFIED

A. Collision Densities

Consider a fuel rod of radius R and infinite length, as in Figure 1, which is subjected to a hemispherically symmetric neutron bombardment. Let j be the constant neutron current density per unit solid angle at the surface of the fuel rod. The number of neutrons per unit time incident on the surface element $Rd\theta dZ$ which are directed toward the volume element dV is then $j Rd\theta dZ \cos \psi dS / (\rho^2 + Z^2)$ where dS is the projection of dV on the plane perpendicular to the line of flight. The probability of penetration to dV is $\exp(-\sum \sqrt{\rho^2 + Z^2})$, and the probability of collision in dV is $\sum \frac{dV}{dS}$. Since $\cos \psi$ equals $(R - r \cos \theta) / \sqrt{\rho^2 + Z^2}$, one can write

$$(1) \quad \bar{D}_0(r) = 4 j \sum R \int_{\theta=0}^{\pi} \int_{Z=0}^{\infty} \frac{(R - r \cos \theta) e^{-\sum \sqrt{\rho^2 + Z^2}}}{(\rho^2 + Z^2)^{3/2}} dZ d\theta$$

for the collision density, $D_0(r)$, of neutrons of the zeroth generation. Integration over Z yields

$$(2) \quad D_0(r) = 4 j \sum R \int_0^{\pi} \frac{(R - r \cos \theta) K_{1/2} \left[\sum (R^2 + r^2 - 2Rr \cos \theta)^{1/2} \right]}{R^2 + r^2 - 2Rr \cos \theta} d\theta$$

where ρ^2 has been replaced by $R^2 + r^2 - 2Rr \cos \theta$ and $K_n(x) = \int_1^{\infty} \frac{e^{-xt} dt}{t^n \sqrt{t^2 - 1}}$. This integral may be transformed to

$$(3) \quad D_0(r) = 4 \pi j \sum^2 R \left\{ -\frac{r}{R} K_0(\sum R) I_1(\sum r) - K_1(\sum R) I_0(\sum r) \right. \\ \left. + \left(1 - \left[\frac{r}{R}\right]^2\right) \int_{\sum R}^{\infty} I_0\left(\frac{r}{R} t\right) K_0(t) dt + \frac{r}{R} \int_{\sum R}^{\infty} \frac{I_1\left(\frac{r}{R} t\right) K_0(t) dt}{t} \right\}$$

DECLASSIFIED

Considering the solid angle subtended by dV , the probability of neutron penetration to dV , and the probability of collision in dV , one finds

$$(4) \quad D_n(r) = \frac{\sum_s}{\pi} \int_{r'=0}^R \int_{\theta=0}^{\pi} r' D_{n-1}(r') \frac{K_{11} \left[\sum (r^2 + r'^2 - 2rr' \cos \theta)^{1/2} \right]}{(r^2 + r'^2 - 2rr' \cos \theta)^{1/2}} d\theta dr'$$

$$(5) \quad = \frac{\sum_s}{\sum} \left\{ \frac{1}{r} \int_0^r r' D_{n-1}(r') dr' \left(\int_{\sum r}^{\infty} dt I_0 \left(\frac{r'}{r} t \right) K_0(t) \right. \right. \\ \left. \left. + \int_r^R D_{n-1}(r') dr' \left(\int_{\sum r'}^{\infty} I_0 \left(\frac{r}{r'} t \right) K_0(t) dt \right) \right\}$$

for the collision density of the n th generation.

B. Collision Probabilities

The probability, P_0 , that a neutron of the zeroth generation suffer at least one collision is one minus its probability of escape. The latter probability can be calculated by considering the number of neutrons passing through dA per unit solid angle per unit time in the ψ direction. This is $j \, dA \cos \psi$; thus the number of neutrons in the increment of solid angle subtended by $Rd\theta dZ$ is $j \, dA \, Rd\theta dZ \cos^2 \psi / (\rho^2 + Z^2)$.

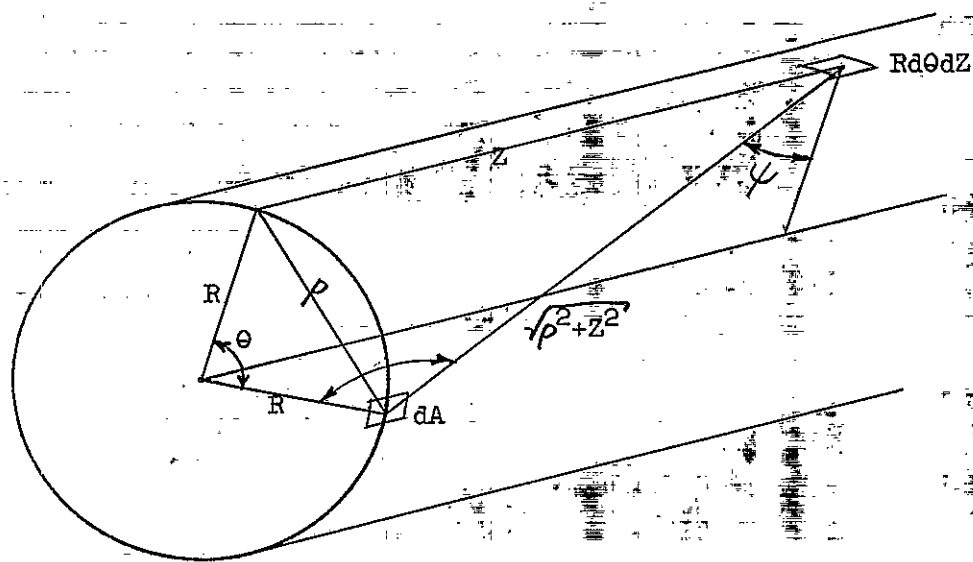


Figure 3

DECLASSIFIED

HW-31351

The probability of escape for these neutrons is $\exp(-\sum \sqrt{\rho^2 + z^2})$; therefore the average probability of escape for the whole generation is

$$(6) \quad 1 - P_0 = \frac{\int_{\theta=0}^{\pi} \int_{z=0}^{\infty} \frac{\cos^2 \psi e^{-\sum \sqrt{\rho^2 + z^2}}}{\rho^2 + z^2} dz d\theta}{\int_{\theta=0}^{\pi} \int_{z=0}^{\infty} \frac{\cos^2 \psi}{\rho^2 + z^2} dz d\theta}$$

In this case

$$\cos \psi = \frac{\rho^2}{2R\sqrt{\rho^2 + z^2}}$$

and

$$\rho = 2R \sin \frac{\theta}{2}$$

thus one obtains

$$(7) \quad P_0 = 1 - \frac{4}{\pi} \int_0^{\pi/2} \sin \theta K_1(2\sum R \sin \theta) d\theta$$

For generations younger than the zeroth, the collision probability P_n of the n th generation can be found, given $D_{n-1}(r)$, by proceeding in a manner similar to that above. By referring to Figure 1, one writes

$$(8) \quad P_n = 1 - \frac{\int_{r=0}^R \int_{\theta=0}^{\pi} \int_{z=0}^{\infty} \frac{rD_{n-1}(r) \cos \psi e^{-\sum \sqrt{\rho^2 + z^2}}}{\rho^2 + z^2} dz d\theta dr}{\int_{r=0}^R \int_{\theta=0}^{\pi} \int_{z=0}^{\infty} \frac{rD_{n-1}(r) \cos \psi}{\rho^2 + z^2} dz d\theta dr}$$

After expressing $\cos \psi$ and ρ in terms of r , θ , and z the equation reduces to

$$(9) \quad P_n = 1 - \frac{\int_{r=0}^R \int_{\theta=0}^{\pi} \frac{rD_{n-1}(r)(R-r \cos \theta) K_1 \left[\sum (R^2 + r^2 - 2Rr \cos \theta)^{1/2} \right]}{R^2 + r^2 - 2Rr \cos \theta} d\theta dr}{\int_{r=0}^R rD_{n-1}(r) dr}$$

DECLASSIFIED

DECLASSIFIED

HW-31351

From Part A, one recognizes that

$$(10) \quad P_n = 1 - \frac{\int_0^R r D_0(r) D_{n-1}(r) dr}{4\pi \int_0^R r D_{n-1}(r) dr}$$

C. Blackness

The blackness of the fuel rod (by definition the ratio of the number of neutrons absorbed in the fuel rod to the number of neutrons entering the fuel rod) may be calculated from the collision probabilities of each

generation; thus $\beta = \frac{\sum a}{\sum} P_0 + \frac{\sum a}{\sum} \frac{\sum s}{\sum} P_0 P_1 + \frac{\sum a}{\sum} \left(\frac{\sum s}{\sum}\right)^2 P_0 P_1 P_2 + \dots$

where $\left(\frac{\sum s}{\sum}\right)^n P_0 P_1 \dots P_n$ is the fraction of the total number of neutrons that are in the $(n+1)^{th}$ generation and $\frac{\sum a}{\sum} P_{n+1}$ is the probability of absorption of those neutrons.

D. Average Angle of Escape

The angle ψ in Figure 3 which appears in the calculation of P_0 is the angle of escape for neutrons of the zeroth generation; henceforth it will be called ψ_0 . The average value of this angle, $\overline{\psi_0}$, can be calculated most conveniently from the secant. Weighting $\sec \psi_0$ with the number of neutrons escaping in the ψ_0 direction, one obtains

$$(11) \quad \overline{\sec \psi_0} = \frac{\int_{\theta=0}^{\pi} \int_{z=0}^{\infty} \sec \psi_0 \frac{\cos^2 \psi_0 e^{-\sum \sqrt{\rho^2 + z^2}}}{\rho^2 + z^2} dz d\theta}{\int_{\theta=0}^{\pi} \int_{z=0}^{\infty} \frac{\cos^2 \psi_0 e^{-\sum \sqrt{\rho^2 + z^2}}}{\rho^2 + z^2} dz d\theta}$$

which reduces to

$$(12) \quad \overline{\sec \psi_0} = \frac{4}{\pi(1-P_0)} \int_0^{\pi/2} K_{12}(2\sum R \sin \theta) d\theta$$

DECLASSIFIED

For generations younger than the zeroth

$$(13) \quad \frac{1}{\sec \psi_n} = \frac{\int_{r=0}^R \int_{\theta=0}^{\pi} \int_{z=0}^{\infty} \sec \psi_n \frac{D_{n-1}(r) r \cos \psi_n e^{-\sum \sqrt{\rho^2 + z^2}}}{\rho^2 + z^2} dz d\theta dr}{\int_{r=0}^R \int_{\theta=0}^{\pi} \int_{z=0}^{\infty} \frac{D_{n-1}(r) r \cos \psi_n e^{-\sum \sqrt{\rho^2 + z^2}}}{\rho^2 + z^2} dz d\theta dr}$$

$$(14) \quad = \frac{R D_n(R)}{\sum_s (1-P)_n \int_0^R r D_{n-1}(r) dr}$$

In terms of the blackness and the collision probability and average angle of escape of neutrons in each generation, one writes

$$(15) \quad \bar{\psi} = \frac{(1-P_0) \bar{\psi}_0 + \sum_s P_0(1-P_1) \bar{\psi}_1 + \left(\sum_s\right)^2 P_0 P_1 (1-P_2) \bar{\psi}_2 + \dots}{1 - \beta}$$

for the average angle of escape for neutrons of all generations,

$\left(\sum_s\right)^n P_0 P_1 \dots P_{n-1} (1-P_n) / (1 - \beta)$ being that fraction of neutrons which escape during the nth generation.

E. Thermal Flux

If $\phi(r)$ is the thermal flux, then

$$(16) \quad \phi(r) = \lambda \sum_{n=0}^{\infty} D_n(r)$$

where λ is the mean free path of thermal neutrons in the fuel rod.

III. Conclusion

Since $D_n(r)$ will rapidly decrease and become less dependent on r as n increases, it is expected that P_n and ψ_n will approach a limit allowing one to calculate the blackness, the average angle of neutron escape, and the flux distribution in the fuel rod. The results thus obtained will be free from the defects inherent in a diffusional treatment; therefore

DECLASSIFIED

HW-31351

it seems profitable to evaluate the intractable integrals above for several generations by IBM methods. It should be noted that this method converges most rapidly for $\frac{\Sigma_a}{\Sigma} \gg \frac{\Sigma_s}{\Sigma}$. This is exactly the domain where diffusion theory is least applicable.

Computations for Transport Theory - G. M. Muller

The method of successive generations⁽¹⁾ requires the evaluation of a large number of integrals whose integrands involve the modified Bessel functions $K_0(x)$ and $K_1(x)$ and the closely related functions $Ki_n(x)$. Several of the integrals involved may be evaluated by means of power series whose coefficients involve the recently tabulated functions $Kj_n(x)$ ⁽²⁾. As an example, the in-

tegral $F(x,t) = \int_0^\infty I_0(tu)K_0(u)du$ may be computed in the form

$$\sum_{m=0}^{\infty} \frac{\gamma_{2m}}{\gamma_{2m+1}} t^{2m} = \sum_{m=0}^{\infty} \frac{1}{\gamma_{2m+1}} Kj_{2m}(x)(tx)^{2m}$$

where

$$\gamma_n = 2^{n-1} \left[\Gamma\left(\frac{n+1}{2}\right) \right]^2 = (n-1)^2 \gamma_{n-2}$$

Since the functions $Kj_n(x)$ are available on IBM cards, it appears quite feasible to tabulate integrals like $F(x,t)$ as two-parameter functions over a range of the parameters sufficient to cover almost any reasonable solid-slug design now under investigation or likely to be proposed in the future. A definitive tabulation of this sort is less expensive than a series of piecemeal computations carried out in connection with the study of each particular slug design; moreover, once the tabulation is completed, the method of Stuart and Woodruff can be applied to each new slug design without an undue amount of tedious calculation. It is also worth noting that several of the integrals which we propose to tabulate are involved in the calculation of the fast effect for cylindrical rods (CP-644).

(1) G. W. Stuart and R. W. Woodruff, "Calculation of Thermal Neutron Behavior in a Solid Cylindrical Fuel Rod", this Quarterly Report.

(2) G. M. Muller, Table of The Function $Kj_n(x) = \frac{1}{x^n} \int_0^x u^n K_0(u) du$, HW-30323.

DECLASSIFIED

DECLASSIFIED
HW-51351

The Solution of Boltzmann's Equation with the Aid of Functions Orthogonal on a Hemisphere - W. A. Horning

A method for solving the Boltzmann equation which is frequently used is the "method of spherical harmonics". This involves writing

$$(1) \quad \phi = \sum_n A_n P_n(\mu), \quad \mu = \cos \theta$$

where ϕ is the thermal neutron flux, $P_n(\mu)$ is a Legendre polynomial and the A_n are constants to be determined. μ is the cosine of a colatitude, θ , which varies from 0 to π .

The author has looked into extensions of this method in which the neutron flux is written in the form

$$(2) \quad \phi = \begin{cases} \phi_+, & \cos \theta > 0 \\ \phi_-, & \cos \theta < 0 \end{cases}, \quad \begin{aligned} \phi_+ &= \sum_n A_{n+} P_n(\cos 2\theta) \\ \phi_- &= \sum_n A_{n-} P_n(\cos 2\theta) \end{aligned}$$

As in (1), θ is here the colatitude of the direction of an elementary pencil of neutrons with respect to an axis parallel to $\nabla\phi$. The interest in the expansion (2) arises from the fact that, in contrast to (1), it is capable of a rapid or even discontinuous variation with respect to θ in the neighborhood of $\theta = \pi/2$, even when the expansion is broken off after a few terms. There is evidence that ϕ is indeed a rapidly varying function of angle near $\theta = \pi/2$. We may therefore expect that the expansion (2) will converge more rapidly than (1). The expansion, similar to (2), on page 101 of Kourganoff⁽¹⁾ has also been studied.

This work should be of use in predicting or interpreting the thermal neutron flux near a uranium-graphite interface.

Measurement of Uranium Resonance for Use in Small-Source Theory - R. K. Cole

According to the small-source model of an infinite graphite pile containing rod of uranium, the thermal flux is

1. Kourganoff, Basic Methods in Transfer Problems.

DECLASSIFIED

$$\phi_{Th}(\rho) = \sum_{\text{all rods}} \frac{Q_1 K_0 (\lambda |\rho - \rho_1|)}{2\pi D} + \sum_i h Q_1 \frac{\left\{ K_0 (\lambda |\rho - \rho_1|) - K_0 \left(\frac{|\rho - \rho_1|}{\sqrt{\theta}} \right) \right\}}{2\pi \theta D \left(\frac{1}{\theta} - \lambda^2 \right)}$$

$$= \sum_i \left[\operatorname{erf} \frac{\left(e^{-a^2/4\theta_0} + \sum_{l \neq i} e^{-\frac{|\rho_i - \rho_l|^2}{4\theta_0}} \right)}{4\pi D \theta_0 (\theta - \theta_0) \left(\frac{1}{\theta - \theta_0} - \lambda^2 \right)} Q_1 \left\{ K_0 (\lambda |\rho - \rho_1|) K_0 \left(\frac{|\rho - \rho_1|}{\sqrt{\theta - \theta_0}} \right) \right\} \right]$$

where

Q_1 = sink strength of the uranium rod

$h = \eta e$

$\frac{1}{\lambda}$ = diffusion length in graphite

θ = Fermi age to thermal

θ_0 = Fermi age to uranium resonance

ρ = position vector

ρ_1 = position of the "i"th rod

a = radius of the uranium rod

λ = resonance absorption factor

$\theta - \theta_0$ = age from resonance to thermal

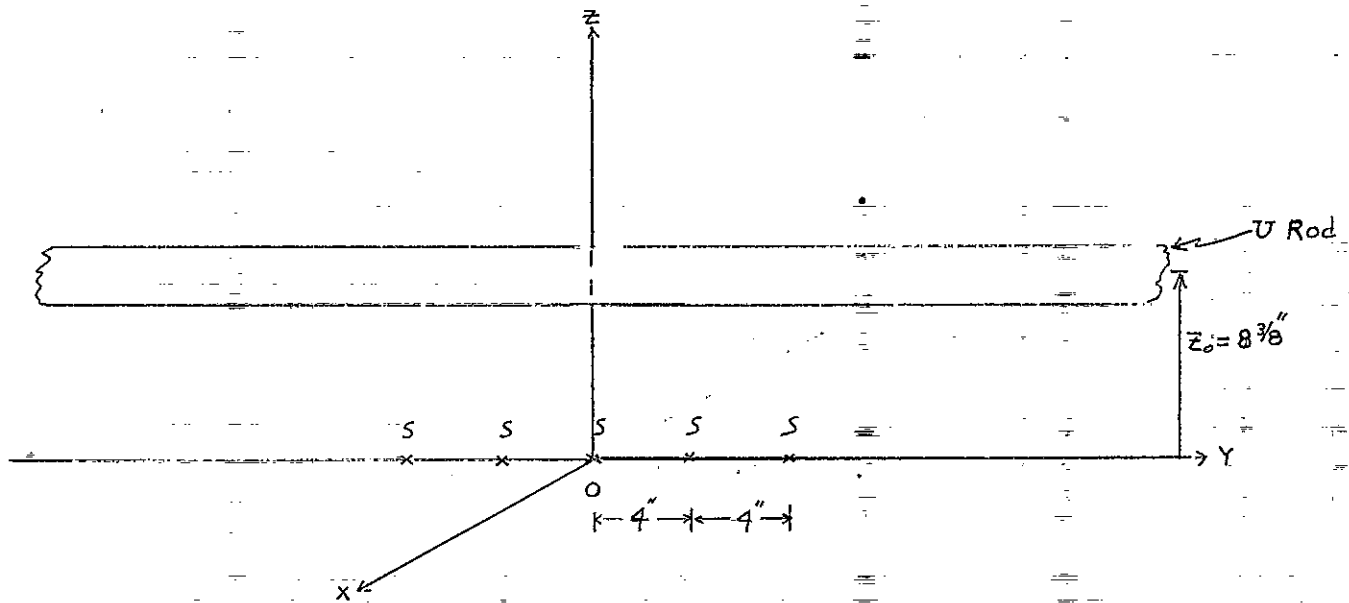
In deriving this expression, the resonance absorption is assumed to be proportional to a delta function at energy E_0 . A simple modification is required if one wishes to take into account two or more distinct resonance peaks.

In order to measure λ and $(\theta - \theta_0)$ the following experiment was performed in the sigma pile of the Exponential Physics Sub-Unit. The sigma pile is a large solid cube of graphite in which a process tube may be inserted. Five radium-beryllium sources of equal strength were placed 4 inches apart and in a line 8-3/8 inches below the uranium rod.

DECLASSIFIED

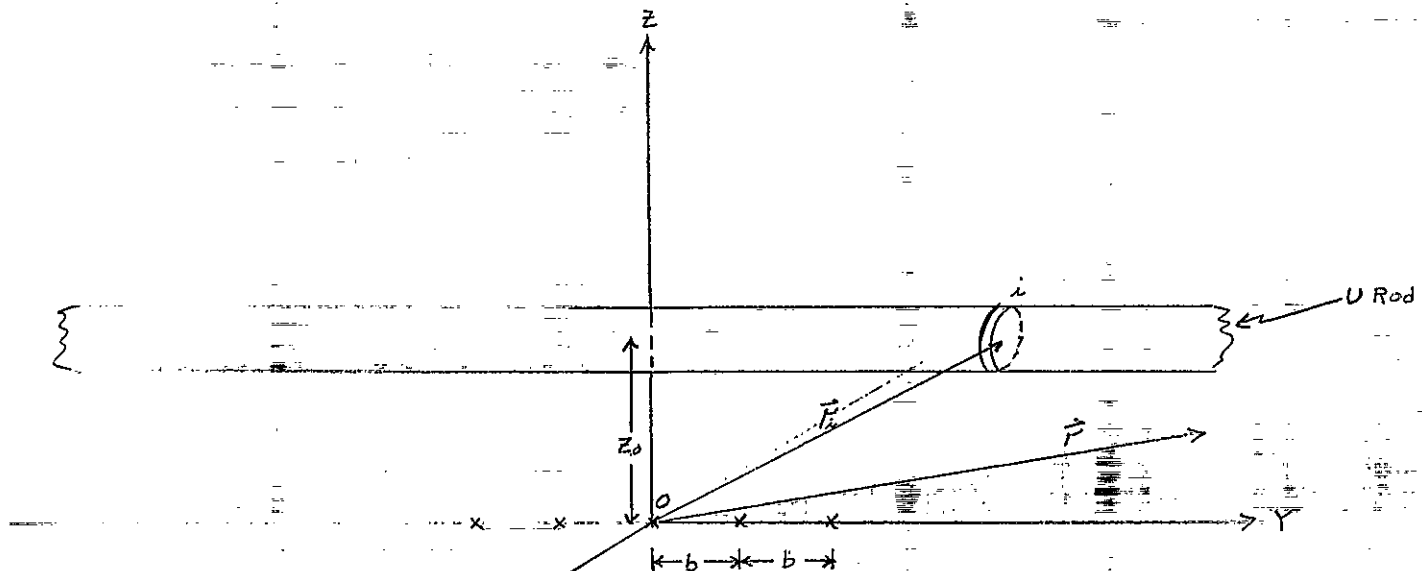
HW-31351

-16-



The uranium was shielded from thermal neutrons by cadmium so that only resonance neutrons would be absorbed by uranium.

Measurements were taken perpendicular to the uranium rod along the line $Z=Z_0$, $y=0$ with cadmium-covered gold foils. Another measurement was made with the sources in the same position but the uranium removed from the process tube. The difference between these two curves gives a measurement of the flux depression by the uranium resonance.



DECLASSIFIED

In the following, let θ be the age to gold resonance.

The slowing down density at r and for $\theta > \theta_0$ is

$$(1) \quad q(r\theta) = \sum_s S_s \frac{e^{-\frac{|r-r_s|^2}{4\theta}}}{(4\pi\theta)^{3/2}} - \int S_1 \frac{e^{-\frac{|r-r_1|^2}{4(\theta-\theta_0)}}}{[4\pi(\theta-\theta_0)]^{3/2}} dy$$

where S_1 is the sink strength,

$$S_1 = 2\pi a \gamma q(\theta_0 r_1)$$

Therefore (1) becomes

$$(2) \quad q(r\theta) = \sum_s S_s \frac{e^{-\frac{|r-r_s|^2}{4\theta}}}{(4\pi\theta)^{3/2}} - 2\pi a \gamma \sum_s \int_{-\infty}^{\infty} S_s \frac{e^{-\frac{|r_1-r_s|^2}{4\theta_0}}}{(4\pi\theta_0)^{3/2}} \frac{e^{-\frac{|r-r_1|^2}{4(\theta-\theta_0)}}}{[4\pi(\theta-\theta_0)]^{3/2}} dy$$

This must also be summed over three ages since the sources emit neutrons in three distinct energy groups.

Then (2) becomes for five-point sources

$$(3) \quad q(r\theta) = \sum_{\theta} \frac{S_{\theta}}{(4\pi\theta)^{3/2}} \left\{ 2 e^{-\frac{(b^2+Z_0^2+X^2)}{4\theta}} + 2 e^{-\frac{(4b^2+Z_0^2+X^2)}{4\theta}} + e^{-\frac{(Z_0^2+X^2)}{4\theta}} \right\} \\ - \sum_{\theta} \frac{S_{\theta} a \gamma}{\theta_0 \sqrt{\theta(\theta-\theta_0)} 16\pi^{3/2}} \left[2 \exp \left\{ \frac{\theta\theta_0(Z_0^2-X^2-4b^2) + 4b^2\theta_0^2 - Z_0^2\theta^2}{4\theta\theta_0(\theta-\theta_0)} \right\} \right. \\ \left. + 2 \exp \left\{ \frac{\theta\theta_0(Z_0^2-X^2-b^2) + b^2\theta_0^2 - Z_0^2\theta^2}{4\theta\theta_0(\theta-\theta_0)} \right\} + \exp \left\{ \frac{\theta\theta_0(Z_0^2-X^2) - Z_0^2\theta^2}{4\theta\theta_0(\theta-\theta_0)} \right\} \right]$$

From the experimental data, a curve was drawn representing the flux depression of the uranium resonance (the second sum on the right of equation (3)). First, a trial-and-error fit was made with two parameters γ and σ ($\sigma = \theta - \theta_0$). Then another fit was made with the four parameters γ' and σ' and γ'' and σ'' , corresponding to two distinct resonance peaks

$$(\sigma' = \theta - \theta_0', \sigma'' = \theta - \theta_0'')$$

Under the assumption of a single resonance peak, the best fit to the data is given by

γ	$\theta - \theta_0$	E_0
2.17	9.0	8.6 ev

Under the assumption of two resonance peaks, the corresponding results are

	γ	$\theta - \theta_0$	E_0
1)	0.71	4.2	6.1
2)	2.53	29	36

Exponential Pile Measurements in Graphite-Uranium Lattices - E. D. Clayton, C. R. Richey and E. Z. Block

I. 1.66" O.D., 1.10" I.D. Hollow Slug

The dry buckling (internal cooling annulus dry) has been measured with these large hollow slugs in four lattices. The results are listed below.

<u>Lattice Spacing</u>	<u>Buckling x 10⁶ cm²</u>
6-3/16"	2.8
7-1/2"	103.0
12-3/8"	14.4
15"	-61.4

The buckling with water in the internal cooling annulus is presently being measured in the same lattices and will be reported at a later date.

II. Effect of Cooling Annulus on Buckling

If better cooling of the aluminum-jacketed uranium slugs can be obtained, then higher pile power levels will be possible. One method of obtaining this objective is to increase the water to uranium ratio per unit of cell by changing the water annulus thickness. The water to uranium ratio (on a molecular basis) in the Hanford reactors at present is about 0.2. For two new piles under construction, the cooling annulus has been increased so that this ratio will be about 50% higher which will permit operation

at a higher power level. The lattices measured under the exponential pile program with external cooling were designed with a water to uranium ratio of about 0.2. The measurements were taken both wet and dry from which information was obtained on the water effect for a series of lattice spacings. Since some designs have been proposed which would have a water to uranium ratio of 4 or 5 times that of the present lattices, a series of measurements have been planned to determine the effect of a greater amount of water on the buckling or reactivity. These experiments should also furnish additional information on the effective water values such as the cross-section and q value (ratio of thermal neutron production per cc in water to that in graphite) which are necessary for the correlation of lattice experiments with theory. The information which has been obtained from these experiments thus far is the result of adding water and displacing graphite since the lattice C/U (atoms) ratio per unit cell was not kept constant, i.e., lattice spacing was unchanged. The first results are for the 0.926-inch diameter slug. Measurements had previously been taken with this slug in the 6-3/16-inch and 7-1/2-inch lattices with a water to uranium atom ratio per unit cell of 0.174. The water volume has been increased by factors of 1.94 and 4.42 and dry and wet measurements taken in both the 6-3/16-inch and 7-1/2-inch lattices. The results of these eight new lattice measurements are listed below where, for convenience, the earlier results are also given.

Lattice Spacing	H_2O/U (atoms)	Buckling $\times 10^6 \text{ cm}^2$		Buckling Diff. $\times 10^6 \text{ cm}^2$
		Dry	Wet	
6-3/16"	0.174	115.0	98.2	16.8
7-1/2"	0.174	95.3	66.4	28.9
6-3/16"	0.338	121.6	89.1	32.5
7-1/2"	0.338	102.7	51.4	51.3
6-3/16"	0.768	103.8	-12.9	116.9
7-1/2"	0.768	89.7	-49.1	138.8

With the 0.926-inch slug, the C/U atom ratio per unit of cell is about 100 in the 6-3/16-inch lattice and about 150 in the 7-1/2-inch lattice. At these C/U ratios of 100 and 150, the water effect is seen to be almost linear within the experimental error of the measurements up to a H_2O/U ratio of 0.338; that is the wet buckling may be expressed in terms

of the dry buckling approximately as: $B_w = B_d - \alpha \left(\frac{H_2O}{U} \right)$. The value of α is about $97 \times 10^{-6} \text{ cm}^{-2}$ for the 6-3/16-inch lattice and about $166 \times 10^{-6} \text{ cm}^{-2}$

for the 7-1/2-inch lattice. In going from a $\frac{H_2O}{U}$ ratio of 0.338 to 0.768, the water effect is seen to deviate considerably from linearity. The water coefficient will have a different value for every slug size and each C/U ratio and is known to change sign at the cross-over point buckling (C/U ratio at which dry and wet bucklings are of same value for a given $\frac{H_2O}{U}$ ratio). It is evident that a number of additional experiments

DECLASSIFIED

HW-31351

are needed concerning the effect of cooling water on the reactivity or buckling in graphite-uranium lattices. The results of additional experiments on this problem will be reported as completed. The results of the correlation of theory to the experimental water results will also be given at a later date upon completion.

III. Cross-Over Buckling

If the buckling is plotted versus the graphite to uranium ratio, then a series of curves is obtained; one for each slug size. Furthermore, it is noted that at a certain C/U ratio the wet and dry bucklings are of the same value. The C/U ratio at which this occurs will be referred to as the cross-over point. This point has a particular importance from the standpoint of safety, since at this point there should be no significant change in the reactivity with the loss of cooling water. If the C/U ratio is decreased from the cross-over value, then the wet buckling will have a higher value than the dry, and a reactor of this design would lose reactivity with the loss of water. For the standard Hanford-slug size (1.36" diameter) the cross-over point occurs at a lattice spacing of about 6.9 inches or C/U ratio of about 59. The buckling value is approximately $66 \times 10^{-6} \text{ cm}^{-2}$. This is a value which is probably too small to permit satisfactory operation of the present-sized Hanford reactors with natural uranium. The 1.17-inch diameter slug has a cross-over point at 6-1/4 inches (C/U ≈ 69.8) and a buckling value of about $89 \times 10^{-6} \text{ cm}^{-2}$, which is large enough to permit satisfactory operation of the present-sized Hanford reactors with natural uranium. This cross-over point is somewhat uncertain however, due to the limited number of measured bucklings, one on either side of the cross-over point. From measurements taken with a 0.926-inch diameter slug, a cross-over point has been estimated by fitting the theory to the measured values and then extrapolating the theoretically predicted values to include the cross-over point. The cross-over point is then seen to be at about 5-1/4 inches (C/U ≈ 74.2). The predicted buckling is about $85 \times 10^{-6} \text{ cm}^{-2}$. In Figure 1, the cross-over point buckling and slug radius are plotted against the C/U ratio at the cross-over point. It should be kept in mind that these curves are somewhat uncertain; however, they do suggest that for a given $\text{H}_2\text{O}/\text{U}$ ratio (≈ 0.2) there is a maximum cross-over point buckling which can not be exceeded for any slug size. This value is seen to be approximately $89 \times 10^{-6} \text{ cm}^{-2}$, and the C/U ratio about 69.8. What the maximum cross-over point will be for a different $\text{H}_2\text{O}/\text{U}$ ratio can not be inferred as yet until more measurements have been taken to determine the water effect on the reactivity.

Correlation of Buckling Measurements and Theoretical Formulas - D. E. Davenport

The exponential measurements being made on graphite-uranium lattices have two basic purposes; (1) to develop methods of accurately predicting the reactivity, conversion ratio, and other lattice constants of any proposed water-cooled, graphite-uranium lattice, and (2) to promote a better understanding of the neutron physics involved, the effective cross sections, neutron temperatures, etc.

DECLASSIFIED

DECLASSIFIED

FIGURE 1

(CARBON/URANIUM) ATOMS PER UNIT CELL

50
60
70
80
90
100

CROSSOVER POINT BUCKLING $\times 10^6 \text{ cm}^2$

CROSSOVER POINT BUCKLING
and
SLUG RADIUS
versus
GRAPHITE-URANIUM
RATIO
at the
CROSSOVER POINT

0.136" slug

slug radius curve

0.926" slug

crossover point buckling curve

0.117" slug

DECLASSIFIED

DECLASSIFIED

The first objective is being pursued through empirically adjusting some of the constants in the simple diffusion theory equations commonly used (Project Handbook, CL-697) to give equations which predict the measured bucklings. The "available parameters" for each slug size are chosen as (1) the ratio of the slug disadvantage factor to the thermal neutron cross section of uranium, $\frac{F(\kappa_0 r_0)}{\sigma_0}$, used in the thermal utilization equation, and (2) the resonance cross

section of uranium, σ_0' , which goes into calculation of resonance escape probability, and (3) $\eta\epsilon$. Since these are all quantities whose value is admittedly subject to question for any lattice, this choice does not seem unreasonable.

The method of selecting parameters to fit the data is to select a value of $\frac{F(\kappa_0 r_0)}{\sigma_0}$ and a series of values for σ_0' and then calculate $\eta\epsilon$ from the equation

$$\eta\epsilon = \frac{B(L^2 + k\tau) + 1}{pf}$$

using the measured values of the bucklings for a given slug size (for which $\eta\epsilon$ should be constant) and a series of lattice spacings. The "best" value of σ_0' is that which will give the minimum variation in $\eta\epsilon$ for the series of lattice

spacings. Then a new value of $\frac{F(\kappa r)}{\sigma_0}$ is chosen and the process is repeated. Since this approach is very long and tedious, if attempted by hand calculation, it was made practical only through the use of the IBM installation at Hanford.

The calculations are still in their early stages, and it is not obvious that the technique will give suitable fits to all slug sizes and lattice spacings investigated. However, the calculations are well enough advanced for the case of the standard Hanford slug (metal diameter 1.36", length 4", aluminum spacers, 0.38") in a dry channel of lattices varying from 6-3/16" to 8-3/8" lattice spacing to indicate the following:

- (1) Values of the parameters can be selected which will accurately (within $2 \times 10^{-6} \text{ cm}^{-2}$) reproduce the experimental buckling measurements in this range.
- (2) One can arbitrarily select one of the three parameters and still find a combination of the other two which will fit the data.

Thus, for preliminary values of L^2 and τ which were selected, the following wide range of constants were found to give an acceptable fit.

DECLASSIFIED

Set	$\frac{F(\lambda_0 r_0)}{\sigma_0}$ ($\times 10^{-24}$)	σ_0' ($\times 10^{24}$)	$\eta \epsilon$	η (assuming $\epsilon = 1.033$)
(1)	0.10	1.20	1.2546	1.2145
(2)	0.15	1.375	1.3052	1.2635
(3)	0.16	1.41	1.3154	1.2734
(4)	0.17	1.445	1.3257	1.2833
(5)	0.19	1.512	1.3460	1.3030
(6)	0.31	1.885	1.4662	1.4194

These results might be expressed in equation form by saying that for an acceptable fit to the data for the one slug size, one chooses the parameters from the equations

$$\eta \epsilon = 1.007 \times 10^{-24} \frac{F(\lambda_0 r_0)}{\sigma_0} + 1.1542$$

and

$$\sigma_0' = 3.263 \times 10^{-48} \frac{F(\lambda_0 r_0)}{\sigma_0} + 0.88 \times 10^{-24}$$

These results are applicable only over the range of measurements, of course.

Calculations are presently in progress for the same slug size and water in the cooling channel and will then be carried out for other slug sizes. It is anticipated that for uranium/moderator ratios much higher than that for the 1.36" slug in the 6-3/16" lattice, the equations will not be adequate because of neutron spectrum and interaction effects. However, these cases are not presently of much interest since the lattice multiplications are less than one for natural uranium.

Exponential Measurements in 4' x 4' Exponential Piles - W. B. Farrand - R.C. Lloyd

I. Relocation of Exponential Facilities

During this quarter about 50% of the equipment, material and personnel of the Exponential Physics Sub-Unit have been moved into the new technical building, 326. Though the actual move from the outer areas was accomplished in about two weeks, considerably more time has gone into getting the scalers and other electronic equipment functioning to the necessary precision, modifying tables, cabinets and other laboratory equipment to suit the new quarters and getting the necessary screens welded over windows, hinges welded in place, and door locks changed to meet security requirements. Since the neutron sources to be used in Building 326 have about 20 times the neutron emission as those previously used in the exponential experiments, new handling procedures and measurement techniques have been developed to make use of the higher available flux without over-exposing the personnel.

II. 4' x 4' Exponential Piles

The first exponential piles built in the 326 Building were the small 4' x 4' piles, previously described (HW-30508) as being of particular interest in that they permit rapid, though rough measurements of the buckling ($\pm 10 \times 10^{-6} \text{ cm}^{-2}$) using only 25% or less as much material as the 8' x 8' exponential units. An 8-3/8" lattice unit has been completed and a 5-3/16" lattice unit is over 50% completed and awaits some special graphite pieces which are currently being machined in the Technical Shops.

The 8-3/8" unit was constructed on a graphite base 37.69" high which has provisions for source placement at the top of the base or in a plane near the middle of the base. This provides flexibility in the length of the thermalizing column above the sources which is useful when the units are used for diffusion length measurements. The lattice portion of the pile is 58-5/8" high giving a lattice section which is 6 cells wide and 9 cells high. The pile is completely covered with cadmium to reduce the thermal neutron exposure of personnel and to prevent the reflection of thermalized neutrons back into the pile from the walls, floor and objects in the room.

III. Polonium-Beryllium Source Calibrations

Eight Po-Be source pellets, having a neutron emission of about 7×10^7 neutrons per second apiece, were purchased to be used in the 4' x 4' exponential pile measurements. These eight sources were paired to make four matching pairs, since such an arrangement makes for the simplest calculation of exponential results when the resulting four sources are placed in a diamond array in the pile base. The total neutron emission of the eight sources was 5.8×10^8 neutrons per second on December 28, 1953 as quoted by the vendor. On this basis, the neutron emission, as of the same date, of the four pairs of sources as recanned and intercompared in a graphite column was:

#1	1.448×10^8
#2	1.449×10^8
#3	1.454×10^8
#4	1.450×10^8

IV. Flux Traverses Within a Lattice Cell of the 8-3/8" Lattice

One of the outstanding advantages of the higher intensity sources available in the 4' x 4' exponential piles is that they make possible a detailed intracell traverse including the slug. Previous attempts at making intracell traverses have always been suspect, since the slug traverse has had to be made in the Test Pile where the high flux was available, but the slug was in a foreign lattice. From accurate intracell traverses, one can calculate the thermal utilization, the lattice diffusion length, and perhaps other lattice constants which would permit a more thorough analysis of the exponential experiments.

To check on the validity of theoretical diffusion length formulas available for heterogeneous lattices, a measurement of the diffusion length and the intracell traverse was made in the 8-3/8" lattice with a dry P-10 (Li-Al alloy) loading replacing the uranium. The details of the traverse in the graphite portion of the cell were measured with 3/4 indium foils. The traverse within the slug was made with 1/4" gold foils with two positions in the graphite being measured to furnish normalization of the two traverses. In the graphite portion of the cell, the traverses were made in both the vertical and horizontal directions from the horizontal P-10 rods and along the cell boundaries. Intermediate points will be obtained by interpolation. The results are presently being calculated.

A horizontal traverse across the entire pile was made and fitted with a cosine series to find the effective size of the 4' x 4' pile. It was found that the effective extrapolation distance was about 1.6" as compared with the theoretical value of about 0.75" for thermal neutrons in graphite. The difference apparently represents the amount of reflection of fast neutrons back into the pile that exists because of the small pile size. This may cause some difficulty with obtaining an accurate diffusion length measurement if it cannot be corrected for.

V. Uranium Lattice Measurements

The eight-foot rods of uranium have been cut to 4-foot lengths and recanned for use in the 4' x 4' pile to permit accurate intracell traverses in the uranium lattices whose bucklings have been measured to date. Materials have also been ordered to permit measurement of U-235, P-10 lattice bucklings and U-235-Th lattice bucklings. A measurement of the intracell traverse in these lattices will also be made.

Physical Constants Testing Reactor⁽¹⁾ - D. J. Donahue, D. D. Lanning

I. Nuclear Safety Considerations

In order to evaluate the hazards to be encountered in the operation of the PCTR, it is necessary to know the behavior of the power level and the period of the reactor as a function of time when various changes are made in its configuration.

The fastest way to introduce excess reactivity into the pile is simply to open the control rods at the maximum possible rate. This maximum speed, in the present design, is limited so that:

$$\frac{dk}{dt} \leq + 3.3 \times 10^{-4} / \text{sec}$$

If, after the pile is critical, the control rod motion is continued at this rate, large amounts of excess k and dangerous periods could be encountered. To determine the power level as a function of time under these conditions, the pile kinetic equation derived by Wallach⁽²⁾ for

1. See Reports HW-30508, HW-27354, and HW-27140
2. Wallach, S., WAPD-13

for the case where $\frac{dk}{dt} = \text{constant}$ has been solved using approximately the parameters of the PCTR. These parameters are:

$$\ell = 10^{-3} \text{ sec}$$

$$\frac{dk}{dt} = 3.75 \times 10^{-4} / \text{sec}$$

where ℓ is the neutron generation time.

The neutron generation time of 10^{-3} seconds is approximate, but probably represents a lower limit to that which might be expected in a graphite-uranium pile. The rate of reactivity increase, $3.75 \times 10^{-4} \text{ dk/sec}$, is slightly greater than the maximum possible in the PCTR. This value was chosen primarily because it is the closest one to the actual case which can be used in Wallach's equation. Both of these numbers, therefore, are pessimistic and the resulting curves represent a slightly worse case than is to be expected in the PCTR. Figure 2 illustrates the solution of Wallach's equation with these conditions. Curve 1 represents the case where the pile is just critical with the control rods closed at $t = 0$. From this condition the rods are opened at the maximum rate.

In curve 2, the pile is subcritical with the control rods closed. If they are then opened at the maximum rate, the curve of power level vs. time has a finite slope at $t = 0$, the time when the pile reaches criticality. $\left(\frac{dn}{dt}\right)_{t=0} = 4$ was chosen as a reasonable number.

Curve 3 gives the equilibrium period of the pile, assuming that it is just critical at $t = 0$ when the rod opening begins. The equilibrium period is that period achieved if, at a particular time, the rod opening is stopped, and time is allowed for the delayed neutrons to reach equilibrium with the rest of the pile neutrons. The values on this curve were obtained from the results of Mills⁽¹⁾.

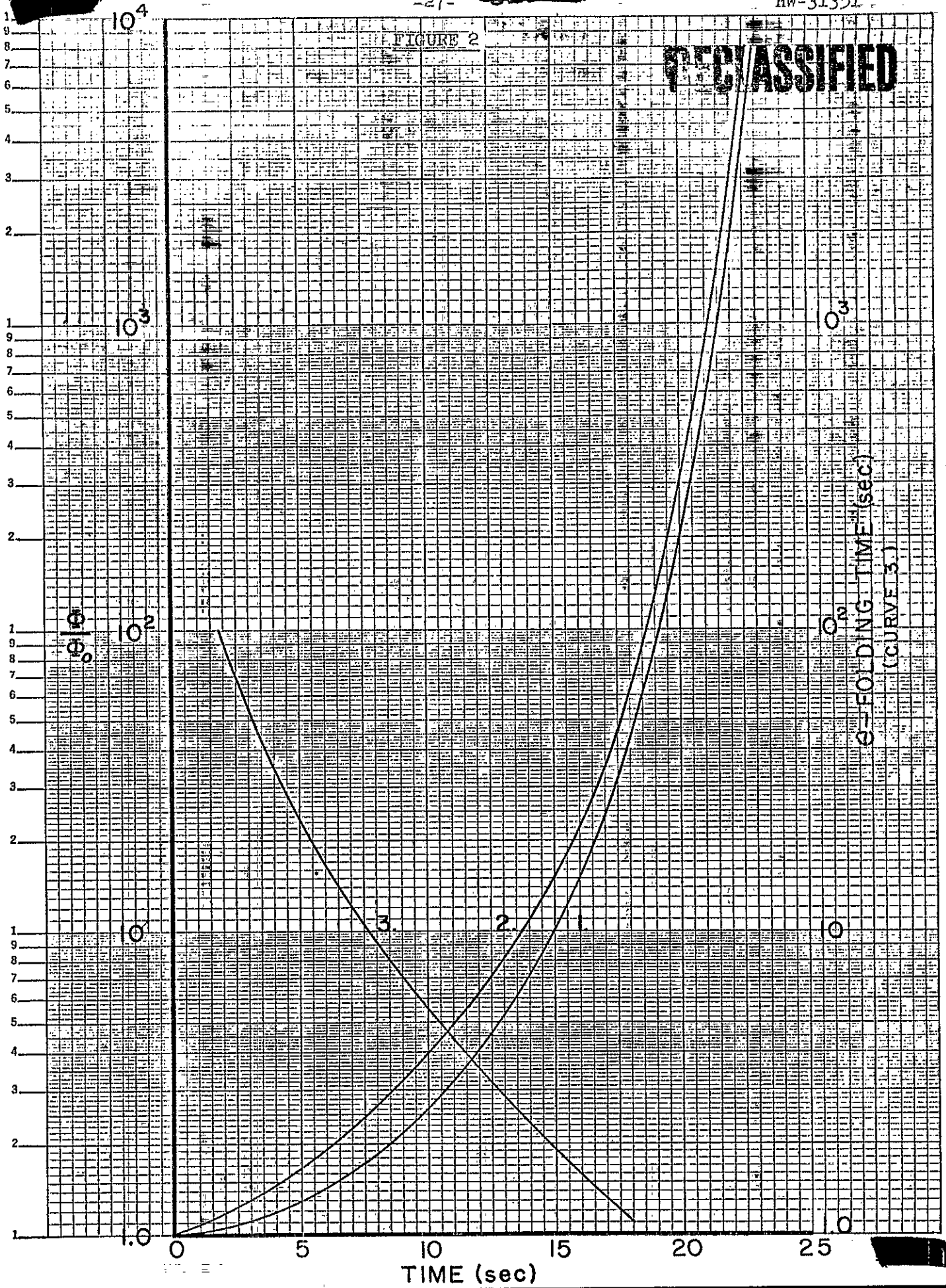
II. Critical Mass of the Physical Constants Testing Reactor

The longitudinal flux along the length of the core of the PCTR will be leveled by the use of an array of movable slugs at the ends of the reactor. Assuming the flux can be leveled in this manner, then to study the necessary critical conditions for the enriched uranium drive rods surrounding the core, the flux can be considered as radially dependent only. The procedures for finding the critical conditions in this case were discussed in the last Quarterly Report⁽²⁾ and will be repeated in part here for convenience.

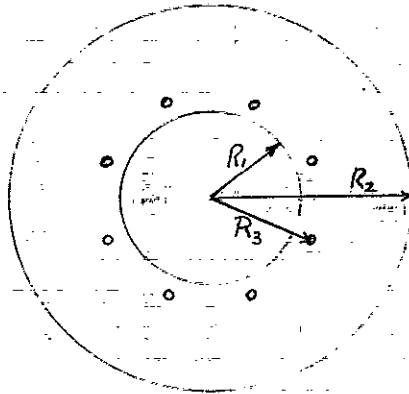
1. Mills, M., TID-71
2. HW-30508, Quarterly Report, Physics Unit, Jan. 11, 1954, D. E. Davenport, J. E. Faulkner, J. Ozeroff.

FIGURE 2

DECLASSIFIED



DECLASSIFIED



R_1 is the radius of the 32 U-235 aluminum alloy driver rods, 51.6 cm.

R_2 is the extrapolation edge of the pile, 125.9 cm.

R_3 is the radius of the eight control rods, 70 cm.

The region inside the driver rods contains the removable core and is assumed to be filled with graphite for this calculation.

The small source equation for the flux (ϕ) is given by

$$(1) \quad D(\nabla^2 - \lambda^2)\phi = \sum_i Q_i \delta(|\vec{r} - \vec{r}_i|) - \sum_i^{\text{driver}} \frac{h_i Q_i e^{-\frac{|\vec{r} - \vec{r}_i|}{L}}}{4\pi\tau}$$

and for this case the solution is

$$(2) \quad \phi(\rho) = \frac{Q_1}{2\pi D} \left[\sum_i^{\text{driver}} K_0(\lambda |\vec{r} - \vec{r}_i|) - \frac{32 I_0(\lambda R_1) K_0(\lambda R_2) I_0(\lambda \rho)}{I_0(\lambda R_2)} \right] \\ + \frac{h_1 Q_1}{2\pi D(1-\lambda^2\tau)} \left[\sum_i^{\text{driver}} K_0(\lambda |\vec{r} - \vec{r}_i|) - \frac{32 I_0(\lambda R_1) K_0(\lambda R_2) I_0(\lambda \rho)}{I_0(\lambda R_2)} - \sum_i^{\text{driver}} K_0\left(\frac{1}{\sqrt{\tau}} |\vec{r} - \vec{r}_i|\right) \right. \\ \left. + \frac{32 I_0\left(\frac{R_1}{\sqrt{\tau}}\right) K_0\left(\frac{R_2}{\sqrt{\tau}}\right) I_0\left(\frac{\rho}{\sqrt{\tau}}\right)}{I_0\left(\frac{R_2}{\sqrt{\tau}}\right)} \right]$$

DECLASSIFIED

HW-31351

$$\begin{aligned}
& - \frac{Q_3}{2\pi D} \left[\sum_1^{\text{control}} K_0(\lambda |\rho - \rho_1|) - \frac{8 I_0(\lambda R_3) K_0(\lambda R_2) I_0(\lambda \rho)}{I_0(\lambda R_2)} \right] \\
& + \frac{h_3 Q_3}{2\pi D(1-\lambda^2 \tau)} \left[\sum_1^{\text{control}} K_0(\lambda |\rho - \rho_1|) - \frac{8 I_0(\lambda R_1) K_0(\lambda R_2) I_0(\lambda \rho)}{I_0(\lambda R_2)} - \sum_1^{\text{control}} K_0\left(\frac{1}{\sqrt{\tau}} |\rho - \rho_1| \right) \right. \\
& \left. + \frac{8 I_0\left(\frac{R_3}{\sqrt{\tau}}\right) K_0\left(\frac{R_2}{\sqrt{\tau}}\right) I_0\left(\frac{\rho}{\sqrt{\tau}}\right)}{I_0\left(\frac{R_3}{\sqrt{\tau}}\right)} \right]
\end{aligned}$$

$1/\lambda$ is the diffusion length in graphite taken as 51.6.

τ is the thermal age in graphite taken as 352.

h is the number of fast neutrons for thermal neutrons absorbed.

This equation is adjusted so that the thermal flux goes to zero at the extrapolated boundary R_2 and any fast leakage out of the edge of the reflector has been neglected. The Q_i represents the total number of neutrons absorbed in the i^{th} rod per unit length and hence

$$(3) \quad Q_i = 2\pi a \beta_i J_1(a)$$

where a is the rod radius, β is the probability that a thermal neutron will be absorbed in the rod if it enters the surface. J_1 is the current into the rod and is taken as:

$$(4) \quad J(a) = \frac{\phi}{4} + \frac{D}{2} \left. \frac{\partial \phi}{\partial \rho} \right|_{\rho=a}$$

Using equation (2) for the flux and applying the boundary condition (3) gives two equations for the Q 's. The equations will be homogeneous in the Q 's and hence the determinant of their coefficients can be set equal to zero, giving the critical condition.

The pile is assumed to be just critical with the control rods "open". As discussed by M. Mills in TID-71, the "open" position of the control rod consists of alternate lengths of uranium and cadmium which are nearly completely absorbing to thermal neutrons. In this "open" position, h_3 and β_3

DECLASSIFIED

of the control rods are estimated to be

$$\beta_3 = 0.93$$

$$h_3 = 0.89$$

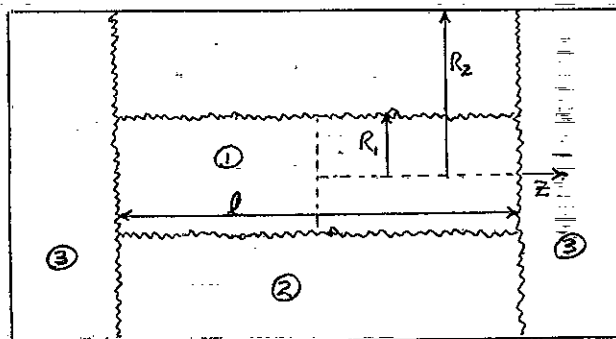
DECLASSIFIED

This leaves only two unknowns in critical condition, h_1 and β_1 of the drivers. Substituting the numbers into the equation gives curve 1 on Figure 3 which is the critical condition for the driver rods.

The driver rods consist of hollow U-235 aluminum alloy slugs which are contained inside a thin steel tube. The outside diameter of the rod is 1-1/2 inches which is the rod radius in the critical calculation. The outside diameter of the uncanned U-235 aluminum alloy slug is 1.277 inches and for this calculation it was assumed to be a hollow slug with an inner diameter of 0.943 inches. By means of a rather complicated calculation involving diffusion theory and estimated transport corrections, it is possible to estimate the values of h_1 and β_1 as a function for various concentrations of U-235 for the assembly of the canned slug in a steel tube. The results of this calculation are plotted as curve 2 in Figure 3. Curve 3 of this figure represents the number of grams of U-235 per cm length of the rod and is plotted versus the blackness of the assembly. The point where curve 1 crosses curve 2 gives the actual critical condition of the driver rods and this corresponds to 0.716 gm U-235 per cm.

The next problem is to estimate the amount of U-235 that must be used in the leveling slugs at the end of the pile in order to give the level flux over the length of the core. This is a difficult problem and has only been solved in an approximate manner by W. A. Horning. His solution is as follows:

Using a one-group calculation the driver region and leveling slug region are assumed to be emitting thermal neutrons to the pile. The effect of the control rods in their open position is taken to be small and is neglected for this case, giving the following approximate picture for a side view of the pile through the center.



DECLASSIFIED

DECLASSIFIED

of the control rods are estimated to be

$$\beta_3 = 0.93$$

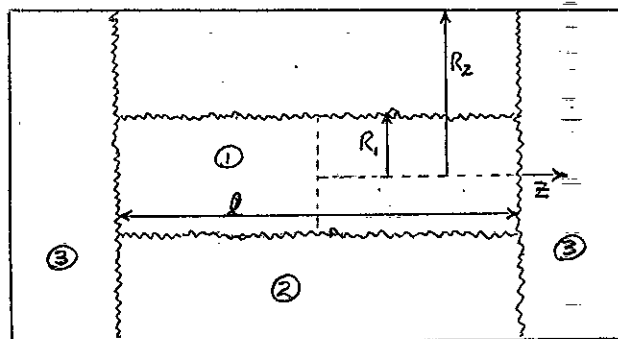
$$h_3 = 0.89$$

This leaves only two unknowns in critical condition, h_1 and β_1 of the drivers. Substituting the numbers into the equation gives curve 1 on Figure 3 which is the critical condition for the driver rods.

The driver rods consist of hollow U-235 aluminum alloy slugs which are contained inside a thin steel tube. The outside diameter of the rod is 1-1/2 inches which is the rod radius in the critical calculation. The outside diameter of the uncanned U-235 aluminum alloy slug is 1.277 inches and for this calculation it was assumed to be a hollow slug with an inner diameter of 0.943 inches. By means of a rather complicated calculation involving diffusion theory and estimated transport corrections, it is possible to estimate the values of h_1 and β_1 as a function for various concentrations of U-235 for the assembly of the canned slug in a steel tube. The results of this calculation are plotted as curve 2 in Figure 3. Curve 3 of this figure represents the number of grams of U-235 per cm length of the rod and is plotted versus the blackness of the assembly. The point where curve 1 crosses curve 2 gives the actual critical condition of the driver rods and this corresponds to 0.716 gm U-235 per cm.

The next problem is to estimate the amount of U-235 that must be used in the leveling slugs at the end of the pile in order to give the level flux over the length of the core. This is a difficult problem and has only been solved in an approximate manner by W. A. Horning. His solution is as follows:

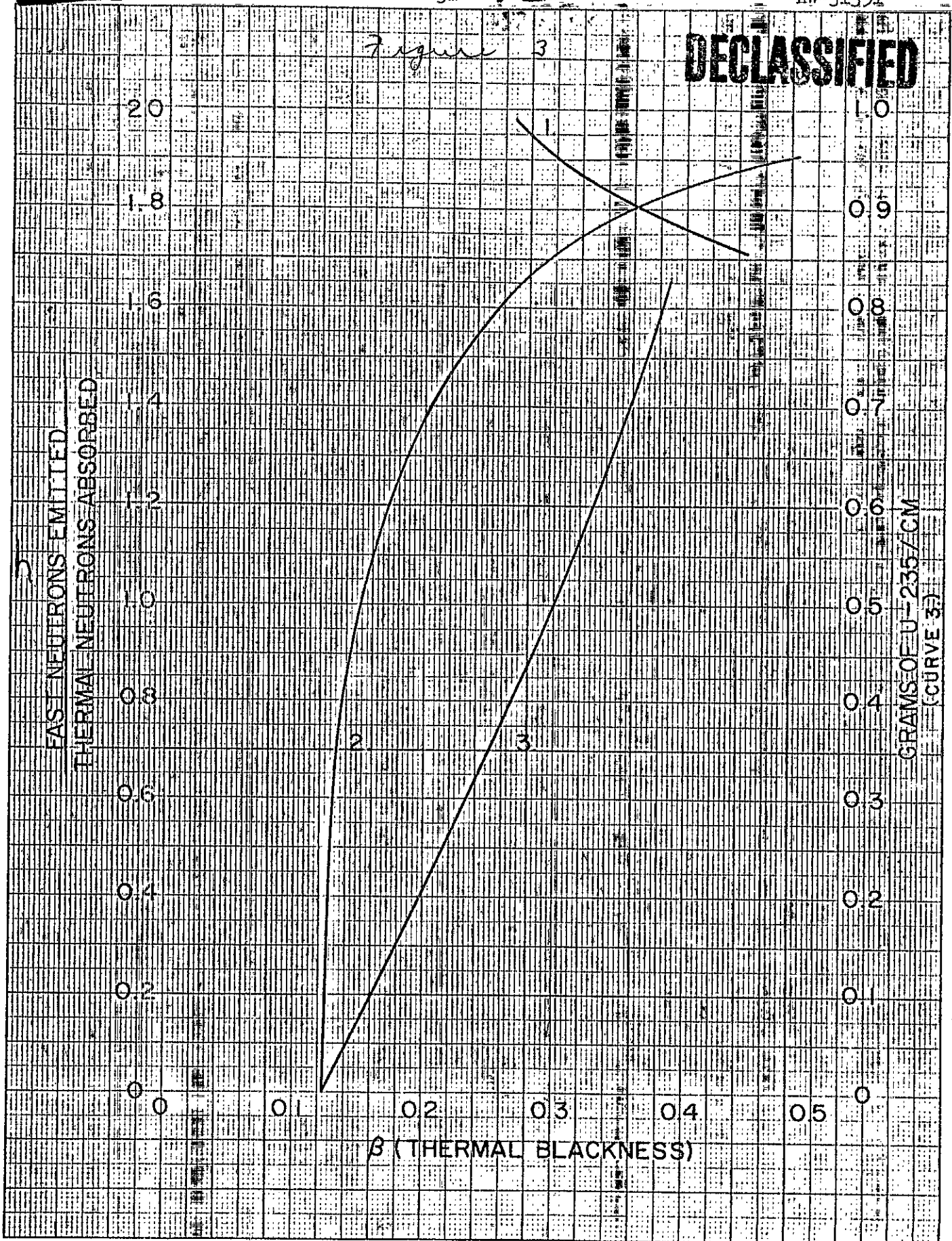
Using a one-group calculation the driver region and leveling slug region are assumed to be emitting thermal neutrons to the pile. The effect of the control rods in their open position is taken to be small and is neglected for this case, giving the following approximate picture for a side view of the pile through the center.



DECLASSIFIED

Figure 3

DECLASSIFIED



DECLASSIFIED

Region (1) is the core region filled with graphite. Region (2) and (3) are graphite reflector regions.

When the leveling slugs are adjusted correctly the flux in a (Z) direction in regions (1) and (2) is constant such that

$$\frac{\partial^2 \phi}{\partial Z^2} = 0$$

Hence for region (1)

$$(5) \quad \phi(\rho, Z) = I_0(\lambda \rho) \quad ; \quad \rho < R_1$$

and region (2)

$$(5) \quad \phi_2(\rho, Z) = \frac{I_0(\lambda R_1) \left[K_0(\lambda \rho) - \frac{K_0(\lambda R_2)}{I_0(\lambda R_2)} I_0(\lambda \rho) \right]}{K_0(\lambda R_1) - \frac{K_0(\lambda R_2)}{I_0(\lambda R_2)} I_0(\lambda R_1)}$$

in region (3)

$$(\nabla^2 - \lambda^2)\phi = 0$$

Using Green's theorem:

$$(6) \quad \int_V (\psi \nabla^2 \phi - \phi \nabla^2 \psi) dv = \int_S (\psi \nabla \phi - \phi \nabla \psi) ds$$

and taking

$$(\nabla^2 - \lambda^2)\psi = 0$$

gives

$$\psi = \frac{\rho - \lambda r}{r}$$

and

$$\int_{V_3-\epsilon} (\psi \nabla^2 \phi - \phi \nabla^2 \psi) dv = \int_{V_3-\epsilon} (\psi \phi - \phi \psi) \lambda^2 dv = 0$$

where ϵ is the very small region surrounding the leveling slugs.

Calling S_1 the surface of a very small region surrounding the point of observation in region (3), it is noted that:

$$\lim_{S_1 \rightarrow 0} \int_{S_1} (\psi \nabla \phi - \phi \nabla \psi) \cdot ds = -4\pi\phi$$

Combining these relations into Green's theorem, equation (5) gives:

$$(7) \quad 4\pi\phi = \int_{S_0} \left(\frac{e^{-\lambda|r-r'|}}{|r-r'|} \nabla \phi(r') - \phi \nabla \psi \right) \cdot ds$$

where S_0 is the surface surrounding region (3).

The source of thermal neutrons/cm²/sec at the leveling slug surface is

$$S(\rho) = -D \frac{\partial \phi}{\partial Z} \Big|_{l/2 + \epsilon} + D \frac{\partial \phi}{\partial Z} \Big|_{l/2 - \epsilon}$$

In regions (1) and (2) $\frac{\partial \phi}{\partial Z} = 0$ for a level flux

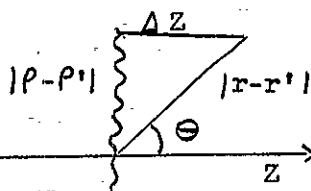
$$\text{hence } \nabla \phi(r) \cdot dS = \frac{\partial \phi}{\partial Z} ds = \frac{S(\rho) ds}{D}$$

or from equation (7)

$$(8) \quad \phi = \frac{1}{4\pi} \int_{S_0} \frac{e^{-\lambda|r-r'|}}{|r-r'|} \frac{S(\rho')}{D} ds - \frac{1}{4\pi} \int_{S_0} \phi \nabla \psi \cdot ds$$

To evaluate

$$\frac{1}{4\pi} \int_{S_0} \phi \nabla \psi \cdot ds$$



$$\cos \Theta = \frac{\Delta Z}{|r-r'|}$$

$$\nabla \psi = \nabla \left(\frac{\rho^{-\lambda |\vec{r}-\vec{r}'|}}{|\vec{r}-\vec{r}'|} \right) = - \left(\frac{\lambda}{|\vec{r}-\vec{r}'|} + \frac{1}{|\vec{r}-\vec{r}'|^2} \right) \rho^{-\lambda |\vec{r}-\vec{r}'|} \hat{r}-\vec{r}'$$

where $\hat{r}-\vec{r}'$ is a unit vector in the direction of $\vec{r}-\vec{r}'$

Thus

$$\frac{1}{4\pi} \int \phi \nabla \psi \cdot d\vec{s} = - \frac{1}{4\pi} \int \frac{\phi \Delta Z}{[|\vec{\rho}-\vec{\rho}'|^2 + (\Delta Z)^2]^{1/2}} \left(\frac{\lambda}{[|\vec{\rho}-\vec{\rho}'|^2 + (\Delta Z)^2]^{1/2}} + \frac{1}{[|\vec{\rho}-\vec{\rho}'|^2 + (\Delta Z)^2]^{3/2}} \right) \rho^{-\lambda [|\vec{\rho}-\vec{\rho}'|^2 + (\Delta Z)^2]^{1/2}} \rho' d\rho' d\phi$$

This function has a zero value for $\Delta Z = 0$ except when $|\vec{\rho}-\vec{\rho}'| = 0$.

Next expanding $\phi(\rho, Z)$ about the point $Z = l/2$, $\rho' = \rho$ rearranging terms in ΔZ , and setting

$$\frac{\vec{\rho}-\vec{\rho}'}{Z} = \vec{\sigma}$$

then

$$\frac{1}{4\pi} \int_{S_0} \phi \nabla \psi \cdot d\vec{s} = - \frac{1}{4\pi} \int \left[\phi(\rho, l/2) + \Delta Z (\vec{\sigma} \cdot \nabla \phi) + \dots \right]$$

$$\frac{1}{(1+\sigma^2)^{1/2}} \left(\frac{\lambda \Delta Z}{(1+\sigma^2)^{1/2}} + \frac{1}{1+\sigma^2} \right) e^{-\lambda \Delta Z (1+\sigma^2)^{1/2}} \sigma d\sigma d\phi$$

now let $\Delta Z \rightarrow 0$ and $|\vec{\rho}-\vec{\rho}'| \rightarrow 0$

in such a manner that $|\vec{\sigma}|$ remains constant

DECLASSIFIED

$$\frac{1}{4\pi} \int_{S_0} \phi \nabla \psi \cdot ds = - \frac{\phi(\rho, l/2)}{4\pi} \int_0^{2\pi} \int_0^\infty \frac{\sigma d\sigma d\phi}{[1+\sigma^2]^{3/2}}$$

$$\frac{1}{4\pi} \int \phi \nabla \psi \cdot ds = - \frac{\phi(\rho, l/2)}{2}$$

Thus the flux in region (3) from equation (8) becomes

$$(9) \quad \phi(\rho, z) = \frac{1}{4\pi} \int_{S_0} \frac{e^{-\lambda|\vec{r}-\vec{r}'|}}{|\vec{r}-\vec{r}'|} \frac{S(\rho')}{D} ds + \frac{\phi(\rho, l/2)}{2}$$

As stated in equation (5), the flux in regions (1) and (2) are known and equations (5) correspond to $\phi(\rho, l/2)$. The problem is to find the value of $S(\rho)$ necessary to satisfy the condition of level flux. This is done in the following manner:

It is desired to solve equation (9) when

$$(10) \quad \phi(\rho, l/2) = \frac{1}{2\pi} \int \frac{e^{-\lambda|\rho-\rho'|}}{|\rho-\rho'|} \frac{S(\rho')}{D} ds$$

where $\phi(\rho, l/2)$ is known and $S(\rho')$ is unknown.

Let

$$\frac{e^{-\lambda|\rho-\rho'|}}{|\rho-\rho'|} = C K_0 (E|\rho-\rho'|)$$

C and E are constants determined by fitting the area and second moments of the two kernels $C = 2\lambda$, $E = \sqrt{2}\lambda$

Then equation (10) becomes

$$(11) \quad \phi(\rho, l/2) = \frac{1}{2\pi} \int_{S_0} 2\lambda K_0 (\sqrt{2}\lambda|\rho-\rho'|) \frac{S(\rho')}{D} \rho' d\rho' d\phi$$

DECLASSIFIED

but this is the solution of the equation

DECLASSIFIED

$$(12) \quad (\nabla^2 - 2\lambda^2) \phi(\rho, l/2) = -\frac{2\lambda}{D} S(\rho)$$

and since $\phi(\rho, l/2)$ in this case is the solution of the equation $(\nabla^2 - \lambda^2)\phi(\rho, l/2) = 0$, then

$$(13) \quad S(\rho) = \frac{D\lambda}{2} \phi(\rho, l/2) ; \quad \rho \neq R_1 \pm \epsilon$$

It is assumed that the leveling slugs are made of the same material as the driver rods and that the driver rods take up a region of the pile having a volume $V_d = 2\pi R_1 b l$ where b is the spacing between the driver rods and l is the length of the rods. Using the results of the driver rod calculation gives a density of U-235 in the driver region of

$$(14) \quad d = \frac{0.716 (32) l}{2\pi R_1 b l}$$

The problem is to use $S(\rho)$ to find the volume of this material needed for the leveling slugs. In order to do this $S(\rho)$ is normalized to the one-group source necessary at the drivers to give the radial flux of equation (5).

Using equation (12)

$$\lim_{\epsilon \rightarrow 0} \left[\int_{R_1 - \epsilon}^{R_1 + \epsilon} 2\pi (\nabla^2 - 2\lambda^2) \phi(\rho, l/2) \rho d\rho = -2\pi \int_{R_1 - \epsilon}^{R_1 + \epsilon} \frac{2\lambda}{D} S_0 \delta(\rho - R_1) \rho d\rho \right]$$

so that

$$(15) \quad \lim_{\epsilon \rightarrow 0} \left\{ \left[\frac{\partial \phi}{\partial \rho} \right]_{R+\epsilon} - \left[\frac{\partial \phi}{\partial \rho} \right]_{R-\epsilon} \right\} = -\frac{2\lambda S_0}{D}$$

but

$$(16) \quad D \left\{ \left[\frac{\partial \phi}{\partial \rho} \right]_{R_1 - \epsilon} - \left[\frac{\partial \phi}{\partial \rho} \right]_{R_1 + \epsilon} \right\} = \text{source of thermal neutrons at } R.$$

Thus the normalizing equation becomes

$$(17) \quad \frac{\text{break in } D \nabla_\rho \phi \text{ at drivers}}{\text{break in } D \nabla_Z \phi \text{ at levelers}} = \frac{2\lambda S_0}{S(\rho)} = \frac{A d b \phi(R_1, l/2)}{A d Z \phi(\rho, l/2)}$$

DECLASSIFIED

where A is a constant containing the fission cross section, number of neutrons per fission, etc., and Z is the length of the leveling slugs measured from the end of the core. The total volume of the leveling slugs is given by

$$(18) \quad V_L = 2 \int_0^{R_2} Z 2\pi \rho a \rho$$

and from equations (13) and (17)

$$Z = \frac{b S(\rho) \phi(R_1, \ell/2)}{2\lambda S_0 \phi(\rho, \ell/2)} = \frac{D b \phi(R_1, \ell/2)}{4 S_0} ; \quad \rho \neq R_1 \pm b$$

at $\rho = R_1$, $S(\rho) = S_0 \delta(\rho - R_1)$ but since in this case there is a width b to the δ function, then

$$S(\rho) = \frac{S_0}{b} \quad R_1 - b < \rho < R_1 + b$$

This gives

$$Z = \frac{1}{2\lambda} ; \quad R_1 - b < \rho < R_1 + b$$

In the actual case, the leveling slugs only extend a distance, R_ℓ , from the center so it is assumed that the rest of the source from R_ℓ to R_2 necessary to make the pile critical is placed into the flux of the driver region. The volume (V_p) of the leveling slugs becomes from equation (18):

$$(19) \quad \frac{V_L}{2} = \frac{D b \phi(R_1, \ell/2)}{4 S_0} (\pi R_\ell^2) + \frac{2\pi R_1 b}{2\lambda} + \frac{2\pi b D}{4 S_0} \int_{R_\ell}^{R_2} \phi(\rho, \ell/2) \rho a \rho$$

The total critical mass (M) is found by using the density (d) given in equation (14).

$$M = V_d d + V_L d$$

Substituting the values of the parameters of the reactor, this procedure gives a total critical mass of 4.4 kg.

In the actual case, aluminum dummy slugs will be used as small spacers between the U-235 aluminum-alloy hollow slugs so that some adjustments can be made on the critical loading. This "bunching" of the U-235 in the driver rods will increase the critical mass. Also, the above calculation neglects any effects of holes drilled in the graphite. This approximation is good for the driver rod calculation, but the leveling slug array will be placed in a region of greatly reduced graphite density on account of the holes. This effective reduction of graphite density should increase the critical mass in the leveling slugs. Hence, the calculated 4.4 kg is expected to be a low estimate; however, it is felt that this calculation can be used as a guide for better understanding of the reactor.

NUCLEAR PHYSICS

Development of a Technique for Measuring the Conversion Ratio for U-233 Production in Exponential Pile Experiments - W. P. Stinson, H. W. Lefevre

In connection with the current examination of the feasibility of producing U-233 in Hanford piles, an attempt is being made to develop a technique for determining the conversion ratio $\frac{\text{U-233 produced}}{\text{U-235 destroyed}}$ for this process. The requirements on the technique are: a) that it shall be usable in a flux of $10^5 \text{ n cm}^{-2} \text{ sec}^{-1}$ attainable in exponential piles, b) that it shall yield at least relative information, i. e., lattice A has a conversion ratio which is larger than that of lattice B by a factor x, and c) that the technique be capable of detecting changes in conversion ratio of 2%.

One technique has been examined during the past quarter. This technique utilizes the activation of the 23-minute Th-233 activity as a measure of U-233 formation, and the counting of fission pulses in a U-235 fission chamber as a measure of U-235 destruction.

It was found experimentally that the natural beta activity of the daughters of Th-232 was larger than the induced Th-233 activity. However, a chemical separation performed by E. E. Voiland reduced this daughter activity by more than a factor of 100. This recently separated thorium should be usable as a detector for about six hours after the chemical separation.

Neutron Spectrometer Facilities - B. R. Leonard, Jr., E. J. Seppi

I. The Energy Variation of Alpha of U-235

The chamber to be used for this experiment has arrived from KAPL where it was built under the direction of F. A. White and his co-workers. This chamber consists of two parts, the first being a parallel plate ionization chamber with a thin enriched boron electrode in which the alpha pulses from the $\text{B}^{10}(\text{n}, \alpha)\text{Li}^7$ reaction are discriminated and used to obtain an accurate $1/v$ response. The second portion of the chamber is a double ionization fission chamber in which two fission foils may be mounted back-to-back to monitor the incident and transmitted intensities through a U-235 transmission disk mounted between the two foils. The

first U-235 fission foil is also to be used to determine the energy variation of the U-235 fission cross section by comparison with the boron (1/v) chamber. This chamber has been mounted, aligned and shielded on the neutron spectrometer and stability tests on the boron chamber are now being performed.

II. Higher Order Corrections

A fission chamber has been used as a detector for a series of transmission measurements of cadmium at low energies. This work is preliminary to work now in progress to attempt to extend the useful range of the spectrometer to neutron energies below 0.020 ev. Figure 4 shows the total cross section obtained for cadmium from 0.020 to 0.20 ev compared to the results of Brockhouse⁽¹⁾. The values obtained before correction for higher order neutrons are also shown for comparison.

A Study of the Error Associated with Neutron Cross Sections Calculated from Empirical Formulas - E. J. Seppi

In determining changes in the reactivity of reactors resulting from changes in neutron temperature, it is necessary to know the neutron cross sections of reactor materials as functions of energy. This change in reactivity is a very sensitive function of some of the cross sections involved, and as a result it is important to know the accuracy of neutron cross sections determined through the use of empirical formulas which were obtained by fitting neutron spectrometer data to proper functional forms.

At neutron energies which are far from nuclear resonance, the Breit-Wigner one-level resonance formula can be expanded in a power series. The neutron cross section of an element is then related to the incident neutron energy, E , by the expression

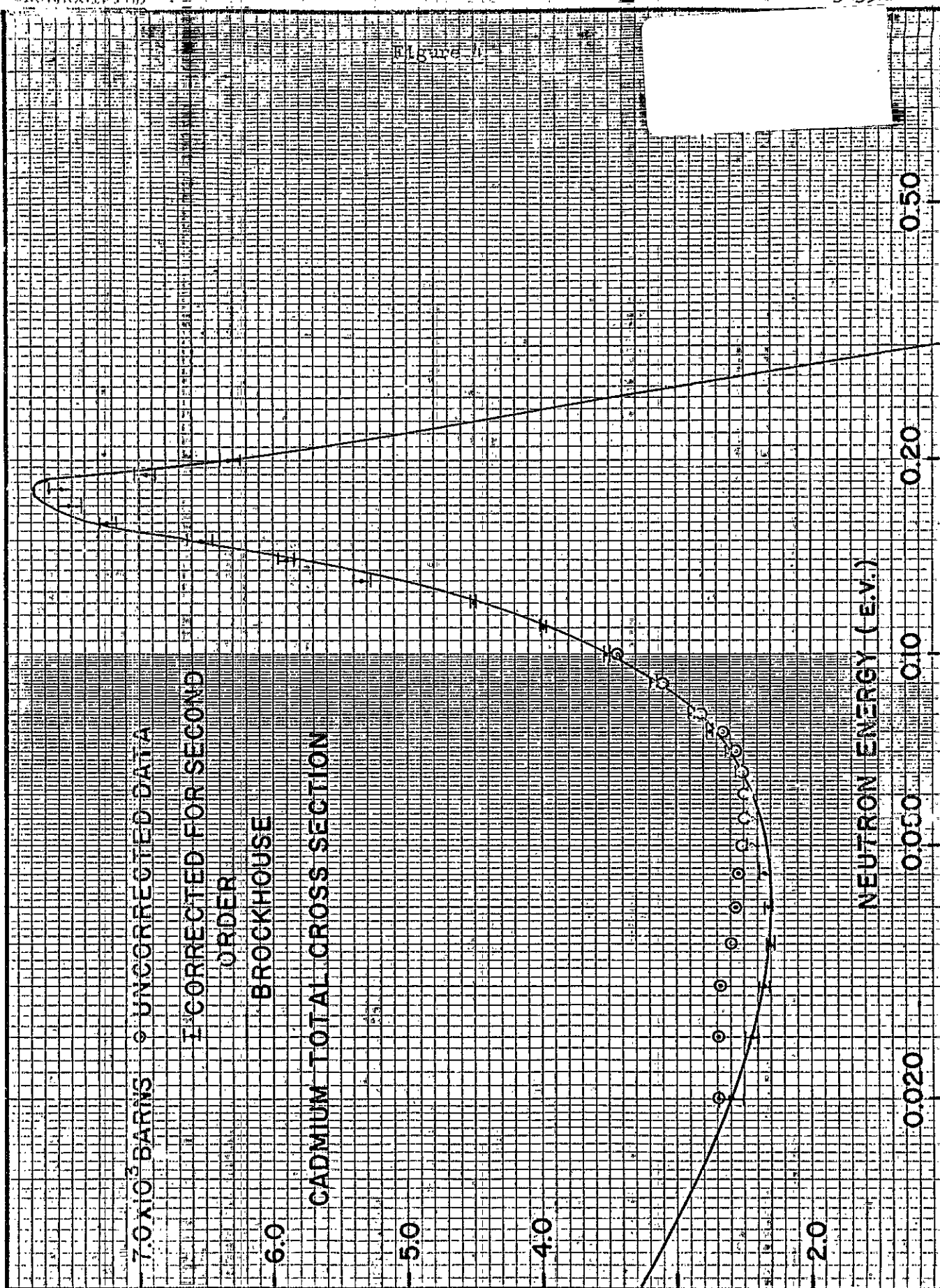
$$(1) \quad \sigma \sqrt{E} = a_1 + a_2 E + a_3 E^2$$

where the approximation is valid in a range $E_1 < E < E_2$ and a_1 , a_2 , and a_3 are constants which can be determined by fitting the equation to experimental data. These data usually give the cross section at various energy points in the range; associated with each point, there is a certain experimental error due to counting statistics. The problem of determining the error in a value of the neutron cross section calculated using equation (1) due to the statistical error associated with the data used to obtain the constants has been investigated and the results are presented below. Because these results can be applied to any case where experimental data are fit to a power series, a general solution will be presented.

1. Brockhouse, B. N., Canadian Journal of Physics, 31, 432 (1953)

Figure 1

Unclassified



UNCLASSIFIED

Unclassified

Suppose a polynomial of the form

$$(2) \quad \bar{y} = a_1 + a_2 X + a_3 X^2 + a_4 X^3 + \dots + a_j X^{j-1}$$

is fit to experimental data consisting of n points $[(y_i \pm \epsilon_{y_i}), X_i] \quad i = 1, 2, 3, \dots, n$ where the a 's are constants to be determined, y_i is the experimentally determined value of y when X is equal to X_i , and ϵ_{y_i} is the statistical error associated with y_i . Each a and consequently, any value of y determined using the resulting empirical equation will have an error associated with it due to the error ϵ_{y_i} . The magnitude of this error can be determined in the following manner.

When the polynomial equation (2) is fit to the experimental data by the methods of least squares, it can be shown that the constants a_q are given by

$$(3) \quad a_q = \frac{\sum_{k=1}^j \sum_{i=1}^n y_i X_i^{(k-1)} D_{kq}}{D}$$

where the terms are defined as follows: Let (y_i, X_i) be given experimental points as discussed above; then D is the determinant whose elements are

$$(4) \quad d_{mn} = \sum_{i=1}^{i=n} X_i^{(n+m-2)}$$

and D_{kq} is the cofactor of the k th row and the q th column of D . Applying the standard methods of the propagation of probable error to equations (2) and (3) gives, respectively,

$$(5) \quad \epsilon_y = \left\{ \sum_{q=1}^{q=j} \left(X^{(q-1)} \epsilon_{a_q} \right)^2 \right\}^{1/2}$$

and

$$(6) \quad \epsilon_{a_q}^2 = \sum_{e=1}^{e=n} \left(\frac{\partial a_q}{\partial y_e} \epsilon_{y_e} \right)^2 = \frac{\sum_{e=1}^{e=n} \left(\sum_{k=1}^{k=j} X_e^{(k-1)} D_{kq} \epsilon_{y_e} \right)^2}{D}$$

where ϵ_{a_q} is the error in a_q due to the statistical error ϵ_{y_i} in y_i and ϵ_y is the error in the value of y calculated using equation (2) where the a 's are given by equation (3).

Simplified expressions were derived for the cases $j = 2$ and $j = 3$. Two simplifying assumptions were made: 1) it was assumed that the error in the experimental points was constant, that is $\epsilon_{y_i} = \epsilon$ for all values of i ; 2) it was assumed that the experimental points were taken at equal intervals ΔX along the X axis such that $X_i = X_1 + (i-1)\Delta X$.

DECLASSIFIED

HW-31351

Using equation (6) ϵ_{a_1} was obtained as a function of α in the transformation $y' = y$, $X' = X - \alpha$. Then noting that for $X = 0$, $\epsilon_y = \epsilon_{a_1}$, the following expressions were obtained. For a straight line fit, $j = 2$,

$$\epsilon_y = \frac{[12 n(X-X_1)^2 - 12 \Delta X(n-1)n(X-X_1) + 2(\Delta X)^2(n-1)(2n-1)n]^{1/2}}{4 X n (n^2 - 1)^{1/2}}$$

and for a quadratic fit, $j = 3$,

$$\epsilon_y = \frac{3\epsilon}{[(\Delta X)^4 n (n-1)(n+1)(3n^2-12)]^{1/2}} \left\{ \begin{aligned} &60 (X-X_1)^4 - 120(n-1) \Delta X (X-X_1)^3 \\ &+ 12(7n^2-15n+7)(\Delta X)^2 (X-X_1)^2 - 12(n-1)(2n^2-5n+2)(\Delta X)^3 (X-X_1) \\ &+ (n-1)(3n^3-9n^2+8n-4)(\Delta X)^4 \end{aligned} \right\}^{1/2}$$

where ϵ_y is the error in y calculated at X using equation (2), ϵ is the absolute error associated with the experimental values of y , X_1 is the abscissa of the first experimental point, ΔX is the interval between the experimental points and n is the number of experimental points. It should be noted that in general these formulas indicate that the error, ϵ_y , at any point is less than the statistical error, ϵ , of the data. Thus providing data are fitted to functions having the proper form, the error in a value obtained from the empirical function will generally be less than the error associated with the data at a given point.

Thermal Neutron Temperatures - R. E. Heineman

In the last Quarterly Report, a suggested method for measuring the "effective temperature" of a Maxwellian distribution in a reactor was briefly described. The Au-198 activity induced in a thick Au-Cd alloy foil is very sensitive to the energy of the neutrons incident on the foil. The probability that a

neutron of energy E is absorbed in Au is $\frac{N_{Au} \sigma_{Au}(E)}{N_{Au} \sigma_{Au}(E) + N_{Cd} \sigma_{Cd}(E)}$. It has

recently been found, however, that the proposed method of normalizing the Au-Cd activity to that induced by unit current of incident neutrons is unsatisfactory. A 1-mil, pure Au foil which would completely cover the surface of the totally absorbing, thick Au-Cd foil was to perform this function. This would be unsatisfactory, in general, for two reasons: 1) by taking the ratio Au-Cd activity to 1-mil Au activity, the sensitivity in neutron temperature is reduced to an impractical limit, 2) though the Au-Cd activity is proportional to current and though the 1-mil Au activity is proportional to flux, both being independent of the incident neutron angular distribution, the ratio of the two activities is dependent upon angular distribution, the ratio of the two activities is dependent upon angular distribution. This result is obtained

DECLASSIFIED

DECLASSIFIED

-43-

HW-31351

because the relationship between flux and current is dependent upon the incident neutron angular distribution.

Alternate possibilities will be considered and any favorable developments will be reported in the future.

C-12 Absorption Cross-Section Measurement - R. E. Peterson

Of the measurements made in determining the thermal neutron absorption cross section of C-12, those remaining are perhaps the most crucial. They are: 1) measurement of the change in C-12 and C-13 abundance ratio in the irradiated carbon samples, to be done by Dr. R. J. Hayden at Argonne National Laboratory, 2) measurement of the change in Li-6 to Li-7 abundance ratio in the irradiated LiI sample, also to be done at Argonne, and 3) measurement of the activity of the cobalt monitor associated with the carbon samples, to be done at Hanford.

During the past quarter, the two carbon samples and their associated cobalt monitor have been removed from the aluminum sample can in which they were irradiated in the Materials Testing Reactor. Due to the high Co-60 activity ($\sim 10^{10}$ d/s), it was necessary to first isolate the cobalt in a separate cask before work on the carbon samples could proceed. (All the sample capsules had been wired together to maintain a fixed position in MTR). During irradiation, the capsules accumulated an appreciable amount of surface contamination which was removed by repeated washing in sulphuric acid-water solution. In order to identify the remainder of the activity, a gamma ray spectrum was obtained from one of the C-12 samples by use of a scintillation spectrometer. Two outstanding peaks were observed at 1.1 and 1.3 mev which are characteristic of Fe-59. This does not appear surprising in view of the fact that iron is one of the impurities present in the unirradiated C-12.

Both carbon capsules were inspected closely for damage at the break-seal and elsewhere but appear to be as sound as before irradiation. Permission to ship the capsules to Argonne National Laboratory has been requested of the AEC and should be forthcoming shortly.

Pu-240 Burnout Experiment - D. J. Donahue, J. E. Faulkner

An experiment has been designed to examine the feasibility of reducing the Pu-240 content of Hanford produced plutonium by irradiating this material in a tailored neutron spectrum. The experiment consists of measuring the relative concentrations of Pu-240 and Pu-239 in a plutonium sample before and after it is exposed to an epithermal flux in the Materials Testing Reactor at Arco, Idaho. Permission to proceed with this irradiation has been granted by the AEC during the past quarter. The pieces to be irradiated are nearing completion.

DECLASSIFIED

DECLASSIFIEDPHYSICS PROBLEMS CONNECTED WITH PLANT OPERATIONThe Dependence of Pu-240 Concentration in Pile-Produced Plutonium on Neutron Flux Level - B. R. Leonard, Jr.

The Pu-240 concentration of plutonium produced by neutron capture in U-238 in a constant neutron flux has been investigated considering the time dependence of the radioactive members of the decay chain. For neutron fluxes greater than about $10^{13} \text{ cm}^{-2} \text{ sec}^{-1}$, the decay time of Np-239 ($T_{1/2} = 2.33 \text{ das}$) becomes a significant fraction of the total irradiation time. For higher neutron fluxes, then increasingly more Np-239 exists in the product at the end of the exposure decaying to Pu-239 after irradiation. This process then leads to small increases in Pu-239 production with increasing neutron flux level for the same exposure and to more significant decreases in the Pu-240 content since the fraction of Pu-239 produced by Np-239 decay after discharge is not available for the production of Pu-240 by neutron capture. By the same process, however, a possible Np-239 radiative capture cross section becomes of importance since this process would yield Pu-240 by the 7.3 minute half-life Np-240. No significant information on the possibility of a slow neutron radiative capture cross section for Np-239 has been found in a literature search.

The time dependent differential equations describing the concentrations of the various members of the decay chain and of Pu-239 and Pu-240 have been set up, solved, and numerical results obtained for representative values of neutron flux level and total integrated exposure. Solutions have been obtained in each case for Np-239 capture cross sections of 0, 100, and 1000 barns. Other values of cross sections were chosen to give general agreement with experimental values of production.

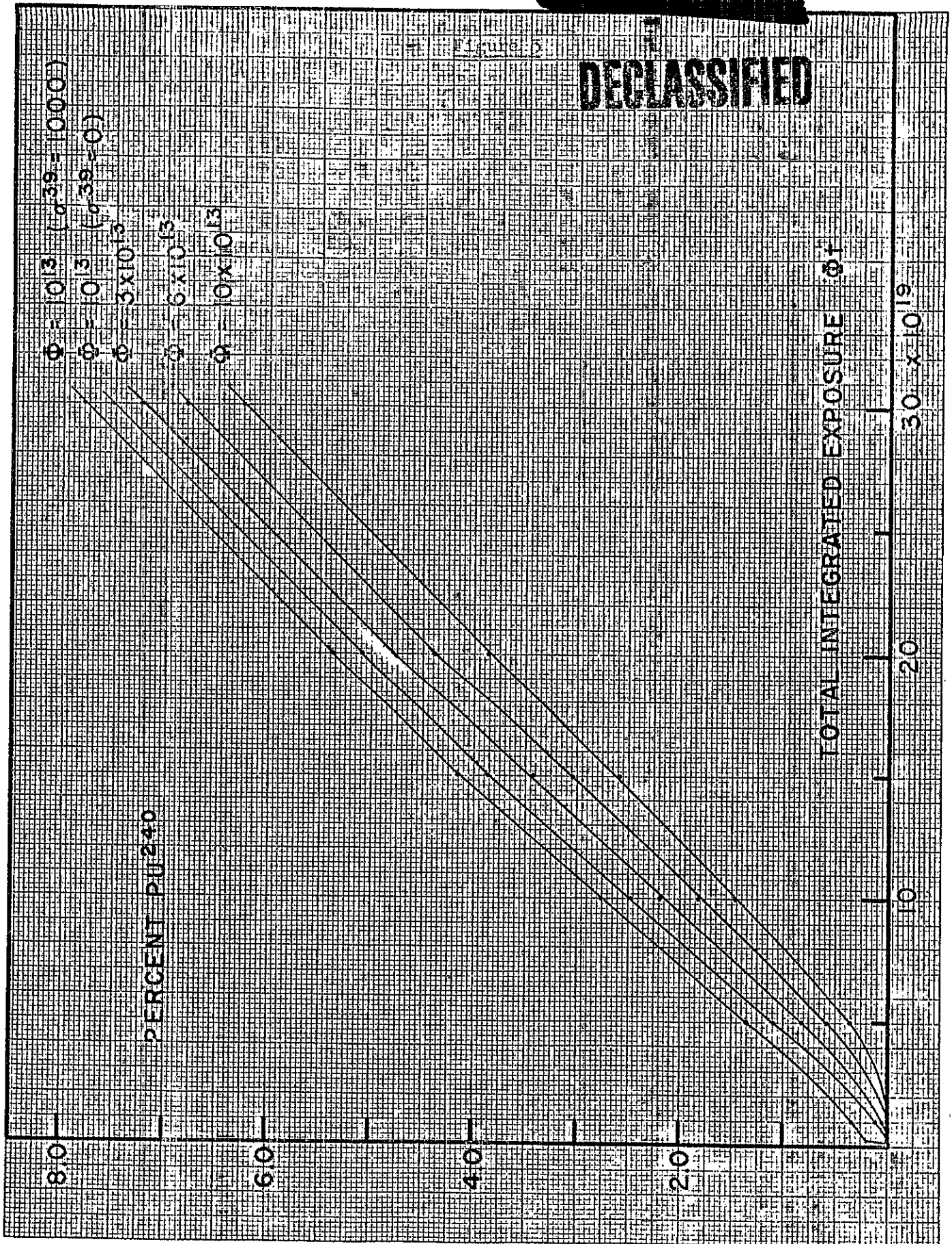
The computations at present have been carried out on a desk calculator and for this reason several simplifications have been made. The most important simplification has been that the calculation of the production of the higher Pu isotopes has not been made. In addition, the Pu-239 produced before discharge and the Pu-240 produced by neutron capture in Pu-239 have been calculated only for the case of zero capture cross section for Np-239. In converting the results of the calculations to percentages, the Pu-239 produced for a finite value of the Np-239 cross section has been corrected by the approximation that the Pu-239 concentration is decreased by the concentration of Pu-240 produced by Np-239 capture.

The calculated percentages of Pu-240 in the plutonium are shown in Figure 5 as a function of total integrated exposure (ϕt). Curves are shown for neutron flux levels of 1, 3, 6, and $10 \times 10^{13} \text{ neutrons-cm}^{-2}\text{-sec}^{-1}$ for a zero Np-239 capture cross section. Also shown is a curve calculated for a flux of 10^{13} and a Np-239 capture cross section (σ_{39}) of 1000 barns. The difficulties attendant with fitting experimental determinations of Pu-240 concentrations to single curves or in the determination of test pile cross-section values from isotopic composition data with accurate knowledge of irradiation flux levels are obvious from these curves.

The importance of possible Np-239 capture cross section may be more clearly seen from the plot of Figure 6, where the calculated Pu-240 concentration is plotted

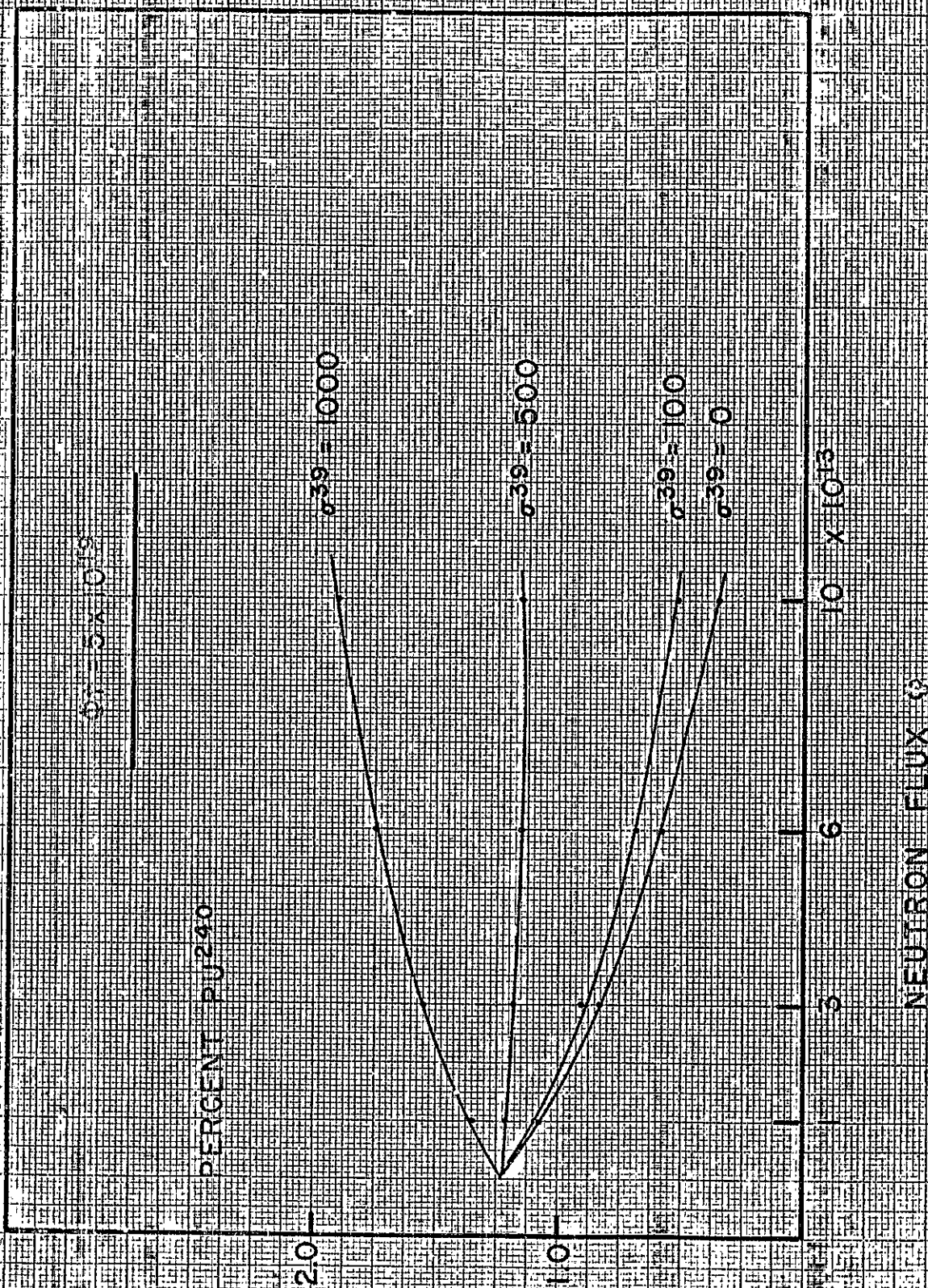
DECLASSIFIED

DECLASSIFIED



DECLASSIFIED

DECLASSIFIED



DECLASSIFIED

DECLASSIFIED

-47-

HW-31351

for values of 0, 100, 500, and 1000 barns for the Np-239 cross section for the same total integrated exposure ($\phi t = 5 \times 10^{19}$ neut/cm²).

A more complete description of these calculations and tabulations of the results has been published in HW-31016.(1)

Neutron Sources - J. O. Erkman

Irradiation of BiF₃ has been proposed as a method of producing a neutron source.(2) Some of the bismuth is converted to polonium; the α -particles from the latter then interact with fluorine to produce neutrons. In order to produce an efficient and stable source, an attempt has been made to solidify the powdered BiF₃ obtained from the vendor by melting the powder. This approach, however, is impractical because of the tendency of the BiF₃ to dissociate at temperatures above its melting point (much of the fluorine has been driven off in all attempts to melt the compound). It is now planned to pack the powder in a thick-walled aluminum can under a pressure of about 6 tons per inch² with a resulting density within 10% of that of solid BiF₃.

As an alternative to the above, the Brush Beryllium Company, using powder metallurgy techniques, is fabricating samples containing bismuth metal and beryllium metal. This type of source in which beryllium serves as the target for the polonium α -particles, should be more efficient than a source containing BiF₃.

Increasing the Subcritical Flux in a Hanford Reactor - J. O. Erkman

The flux in a subcritical reactor is proportional to the neutron source strength in the reactor. It has been shown(3) that the source in a Hanford reactor soon after a shutdown is due primarily to the (γ , n) reaction on deuterium. The magnitude of the subcritical flux is important in determining startup procedures.(4) Safety of operation would be increased, and instrumentation problems would be reduced if this subcritical flux could be increased, perhaps by the addition of beryllium to the reactor.

In order to estimate the amount of beryllium required to increase the flux significantly, the relative yields of neutrons from deuterium (in the form of D₂O in ordinary water) and beryllium (a beryllium salt in water) will be determined. Freshly pushed slugs will be used as the γ -ray source, and indium foils will be used as the detector. The neutron flux in a bucket containing 143 four-inch slugs in the discharge basin at 100-D is sufficient to give a saturated counting rate of 52 counts per second on a 1.0" x 2.5" indium foil, corresponding to

- (1) Leonard, B. R., The Dependence of Pu-240 Concentration in Pile-Produced Plutonium on Neutron Flux Level, HW-31016, March 3, 1954
- (2) Erkman, J. O., A Neutron Source Design which Eliminates Radiochemistry from the Process of Production, HW-29686.
- (3) Kruesi, F. E., Final Report, Production Test 105-58-P, B-Pile Reactivity Under Shutdown Conditions, HW-10559, July 19, 1948.
- (4) Carson, A. B. and Plumlee, K.E., Final Report on PT-105-258-P, Supplement "A", Determination of Residual Neutron Flux at Startup, HW-18058, June 12, 1950.

DECLASSIFIED

DECLASSIFIED

HW-31351

a neutron flux in the neighborhood of 500. This flux is sufficient to make the comparison of the yields of beryllium and deuterium a simple matter. (The flux measurement was made with the assistance of the Special Irradiations Unit and the Exponential Pile Sub-Unit.)

Xenon Reactivity Effects - J. O. Erkman

Document HW-31135, "Notes on Xenon Reactivity Effects in a Hanford Reactor", has been issued. Expressions have been set up so that pile fractions may be used directly to give the reactivity effects of xenon. The equations may be adapted to a reactor using conventional fuel with dimensions or thermal utilization different from present reactors. The power level and flattening parameters have been combined into a single parameter to reduce the number of tables required to cover a given range of operation.

Single Reactor Load for Tritium and Uranium-233 Production - G. W. Stuart

A lattice load composed of alternating N slugs (3.5% Li and 96.5% Al) for tritium production and M slugs (a canned assembly of alternating disks of thorium and Al, Mg, or Zr-25 alloy) for 23 production and nuclear fuel requirements possesses several attractive features:

- a) Thorium is a relatively efficient γ -ray absorber and will, therefore, tend to alleviate the undesirable graphite heating caused by fission product γ radiation. In the conventional method of tritium production employing J slugs (Al-25 alloy), graphite heating is accentuated.
- b) Since the neutron capture cross section of tritium is small, there is little product burnout; hence the most efficient manner in which to manufacture this product is to set the exposure as high as possible. In this we are limited by slug stability and loss of reactivity due to 25 burnout and fission product buildup. The proposed M slug should prove extremely stable because of its excellent heat conductivity, while loss of reactivity would be compensated for by buildup of 23 which yields 2.3 fast neutrons per thermal neutron absorbed as against 2.1 fast neutrons for 25.
- c) Since thorium is a material possessing appreciable resonance cross section, the reactivity of the M-N loading will, because of the doppler effect, possess a metal temperature coefficient far more negative than a J-N loading, thus increasing safety of reactor operation.
- d) Resonance capture of thorium fabricated into M slugs should increase due to increased scattering per thorium atom. This will have a salutary effect on resonance conversion to uranium-233.
- e) The effect of fast fissions in thorium-232 will be enhanced by the intimate arrangement of fuel disks and thorium disks.
- f) Separation of the thorium and fuel disks could be done chemically.
- g) Conversion ratio and uranium-235 investment for the M-N loading scheme compares favorably with alternate loading schemes.

DECLASSIFIED

DECLASSIFIED

-49-

HW-31351

An amplified discussion of this subject may be found in document HW-30839.

Conversion Ratio of Thoria - G. W. Stuart

The Atomic Energy Commission has requested a feasibility report from HAPO on utilizing thoria (ThO_2) instead of thorium metal for uranium-233 production. As one aspect of this problem the change in conversion ratio (nuclei of 23 formed per nucleus of 25 destroyed) generated by such a substitution has been calculated. An exact numerical result is not possible at this time, but the following limits have been obtained.

$$- 0.03 \leq C_{\text{thoria}} - C_{\text{thorium}} \leq 0.01$$

Details of this calculation may be found in document HW-31153.

Conversion Ratio for P-10 Production - R. E. Peterson

Separate yields from four columns which were discharged from DR reactor have been reported. (1) The conversion ratio of tritium production to U-235 depletion has been calculated for each column and is reported as follows:

<u>Tube No.</u>	<u>Total Energy Generated in the Column (MWD)</u>	<u>H³ Yield (Cm³ at NTP)</u>	<u>Conversion Ratio</u>
1474	79.97	1,256	0.48
2573	80.26	1,500	0.57
1875	78.96	1,766	0.68
1966	70.98	1,638	0.70

The H³ yields reported here are an average of two measurements made for each tube. The calculation is based on the assumption that 56 per cent of the total tube energy results from the destruction of 25 in the eleven J pieces in the column and that the energy released per fission is 203 mev. There is good reason to disregard the data from Tube 1474, since it is believed that gas was absorbed in saturating the extraction line. If this is done, then the average conversion ratio of the other three columns is 0.65. This is in good agreement with a previous measurement made on the H-10 loading (0.60 - 0.67), (2) as well as a calculation made from the ratio of average fluxes in the target and fuel slug as determined by foil traverses (0.67).

The desirability of increasing the conversion ratio is obvious and methods for accomplishing this are being studied. Rough estimates of the neutron economy indicate that an increase in the lithium concentration will yield a small increase in conversion ratio. A report will be issued on this work in the near future.

1. Private communication from R. E. Falkoski
2. Peterson, R. E., Conversion Efficiency and U-235 Depletion in H-10, HW-29027

DECLASSIFIED

DECLASSIFIED

Production of Th-234 and Pa-233 - J. T. Russell

In the separation of U-233 from the parent material Th-232, it is of interest to know the expected activity present due to Th-234 and Pa-233. The activity just at the end of radiation will be a function of flux and time, if saturation is not reached. In order to find these functions, the equations were solved assuming only that the burnout of Th-232 was negligible. The equations and solutions may be found in HW-31200. The results indicate that at 90% saturation for a flux of 4×10^{13} n/cm² sec, the Th²³⁴-Th²³² ratio is about 8.2×10^{-8} . The time for 90% saturation is about 7×10^6 sec. Similarly, the 90% saturation ratio for Pu²³³-Th²³² is about 9×10^{-4} which will occur in approximately 8×10^6 sec.

The solution of the complete set of equations leading to U-233 production and the U²³³-U²³⁴ ratio is now underway.

Wide Range Flux Meter - J. T. Russell

In starting up a high-level production pile following a shutdown from full power, it is often advantageous to know just what the flux is at the very beginning of the startup. If this detector would also operate over the entire pile excursion without the necessity of changing ranges, it would be of further advantage. The feasibility of just such a device is now being considered. Interest centers about a fission chamber in a tube of liquid between it and the reflector. The neutron attenuation for such an arrangement could be adjustable from 0 to 10^{10} or more. Now the position might be adjusted automatically so that a constant counting rate is obtained, allowing the power level to be indicated as a function of position.

This meter is described in more detail, along with some applications to automatic control, in HW-31200.

John Ozeroff
Head, Physics Unit
Technical Section
ENGINEERING DEPARTMENT

WJ Ozeroff:as

DECLASSIFIED